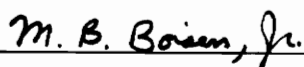# SYSTEMATICS OF BOND LENGTH AND RADII VARIATIONS
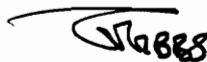# IN FLUORIDE AND SILICATE MOLECULES AND CRYSTALS

by

Jeffrey Scott Nicoll

Thesis submitted to the Faculty of the

Virginia Polytechnic Institute and State University

in partial fulfillment of the requirements for the degree of
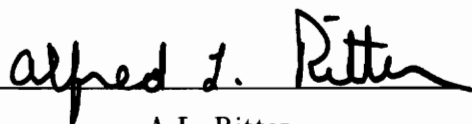
MASTER OF SCIENCE

in

Geological Sciences

APPROVED:

M. B. Boisen, Jr.
M.B. Boisen, Jr., Co-Chairman

Gibbs
G.V. Gibbs, Co-Chairman

alfred l. Ritter
A.L. Ritter

May, 1993

Blacksburg, Virginia

SYSTEMATICS OF BOND LENGTH AND RADII VARIATIONS IN FLUORIDE AND SILICATE MOLECULES AND CRYSTALS

by

Jeffrey Scott Nicoll

(ABSTRACT)

Molecular orbital calculations completed on fluoride molecules containing main group cations have generated bond lengths, R, that match to within $\sim$0.04Å those observed for cation containing coordinated polyhedra in crystals. The calculated bond lengths and those observed for crystals can be ranked with the expression $R = Kp^{-0.22}$, where $p = s/r$, s is the Pauling strength of the bond, r is the row number of the cation and $K = 1.34$. A similar scaling was observed with K values of 1.39, 1.49 and 1.83 respectively for oxide, nitride and sulfide molecules and crystals. Also, the parameter $p = -0.22$ ($\approx \frac{-2}{9}$) is the same as that observed for the oxides, nitrides and sulfides. Furthermore, crystal XY bond lengths, where X represents main–group and transition metal atoms, and Y represents a variety of anions including O, S, N, F, Se and others, agree with XY bond lengths observed in chemically similar molecules to within $\sim$ 0.04Å. There is no difference in correlation between bonds including main–group metal atoms and bonds including transition metal atoms.

Bonded radii for the fluoride ion determined for the molecules increases linearly with bond length, with the variation in bond length being shared equally between the bonded radius of the cation and the anion. Promolecule radii of the metal atom calculated for molecules correlate with metal atom bonded and crystal radii, suggesting that the electron density distribution in hydrofluoride molecules has a largely atomic component.

The bonded radii of Si and O obtained from total electron density maps observed

for coesite and danburite (4–coordinate Si) and stishovite (6–coordinate Si) match those calculated for the monosilicic acid H_4SiO_4 molecule with its four S_4–equivalent SiO bond lengths set successively at values ranging from 1.5 to 1.9Å. These results also demonstrate that for a given bond length, the bonded radii of Si and O are largely independent of their coordination numbers and that the radii of both atoms are nearly the same in both the monosilicic acid molecule and the silicate crystals. The O atoms in danburite are observed to exhibit several distinct bonded radii, ranging between 0.94 and 1.23Å, rather than a single one with each oxide ion exhibiting a different radius along each of the nonequivalent bonds with B, Si and Ca. Promolecule radii calculated for the coordinated polyhedra in danburite agree, to within 0.002Å, with procrystal independent atom model radii obtained in a structure analysis.

ACKNOWLEDGEMENTS

Table of Contents

LIST OF TABLES

vi

LIST OF FIGURES

Chapter 1
BOND LENGTH CORRELATIONS
Introduction

In 1982, Gibbs suggested that a molecule might serve as a useful basis for modeling the bond length and angle variations of a silicate mineral. This suggestion was based on the observation that the separations and angles between the Si and O atoms in the coordinated polyhedra of a number of siloxane molecules are not unlike those in quartz (Gibbs et al., 1972; Tossell and Gibbs, 1978; Newton and Gibbs, 1980; Gibbs et al., 1981; Gibbs and Boisen, 1986; Gibbs et al., 1987a). He also suggested that such models might provide important insight into the forces that govern bond length and angle variations and electron density distributions of the silica polymorphs and silicates in general. The development of such models has since yielded a theoretical basis for the correlation first observed by Smith (1953) between SiO bond length and bond strength sum for melilite and later established for a variety of oxide bond lengths by Baur (1970) and a number of correlations established by Brown and Shannon (1973) between bond strength and bond length. They have also provided a basis for a correlation proposed between SiO bond length and SiOSi angle (Cruickshank, 1961, Brown et al., 1969; Newton and Gibbs, 1980; Boisen et al., 1990).

Since that time, molecular orbital (MO) calculations, completed on a variety of molecules with 4– and 6–coordinated first and second row metal atoms, have generated bond lengths and angles that match those observed, to within a few percent, for chemically similar oxide, sulfide and nitride molecules and crystals (Geisinger and Gibbs, 1981; Julian and Gibbs, 1985, 1988; Gibbs and Boisen, 1986; Gibbs et al., 1987b; Bartelmehs et al., 1989; Buterakos et al., 1992). The close correspondence between observed and calculated bond length data for chemically similar molecules and

1

crystals suggests that the force field that governs bond length and angle variations in a wide range of insulating materials is short ranged and, in large part, independent of the long ranged forces exerted on the coordinated polyhedra by the other atoms of a structure. It also indicates that the force constants and minimum energy SiO bond lengths and SiOSi and OSiO angles calculated for a molecule like $H_6Si_2O_7$ can be viewed as similar to those of a Si_2O_7 group in a silicate and that they can be used to construct a force field. In fact, a potential energy function based in large part on such a force field has been used to generate the structures, the volume compressibilities, the elastic constants and the Poisson ratios for the silicates quartz and cristobalite (Lasaga and Gibbs, (1987; 1988; 1991), Stixrude and Bukowinski (1988); Gibbs et al., (1988), Tsuneyuki et al., (1988), Chelikowsky et al., (1990), Purton et al., (1993) and Boisen and Gibbs (1993)). It has also been used to generate the zero pressure structure of coesite, reproducing both the observed SiO bond lengths to within $\sim$0.01Å and the correlation observed between SiO bond length and SiOSi angle (Stixrude and Bukowinski, 1988; Boisen and Gibbs, 1993). It was also found that when the structures of quartz, cristobalite and coesite are optimized with the potential energy function, assuming triclinic P1 space group symmetry, that the resulting structures exhibit the space group symmetries observed for these three minerals (Boisen and Gibbs, 1993). The success of these calculations not only provides support for the assertion that the nature of the bonding in the Si_2O_7 group in $H_6Si_2O_7$ is similar to that of the group in the silica polymorphs, but it also indicates that the force field of the group plays an important role in governing the properties and the observed space group symmetries adopted by the silica polymorphs.

In this study, MO calculations are completed to learn whether the minimum energy bond lengths calculated for a number of fluoride molecules match those observed

for the coordinated polyhedra in fluoride crystals.

Molecular Orbital Calculations

The MO calculations were completed on $H_{m-n}X^{n+}F_m$ fluoride molecules with m = 3-, 4-, 5- and 6-coordinated first and second row main group metal atoms, X. In the calculations, (1) 6-31G* basis sets were used on the metal atoms and the fluorine atom and a 31G basis set was used on H and (2) ideal geometries (trigonal planar, tetrahedral, trigonal bipyramidal and octahedral fluoride coordinated polyhedra) were assumed with all of the XF bond lengths clamped at one value and with all the HF bond lengths clamped at another. The minimum energy $R(XF)$ and $R(FH)$ bond lengths and the XFH angles were obtained using unrestricted Roothaan-Hartree-Fock self consistent field (SCF) strategies and a quasi-Newton method as employed in GAUSSIAN86 (Frisch et al., 1984).

Discussion

The theoretical minimum energy bond lengths, $R_t(XF)$, calculated for the fluoride molecules (Table 1) are compared in Figure 1 with observed bond lengths, $R_o(XF)$, generated from the crystal radii derived by Shannon (1976). A linear regression analysis of this data yields a slope of 1.13 and intercept of − 0.20. An R^2 value of 0.991 indicates that more than 99% of the variation in $R_o(XF)$ can be explained in terms of a linear dependence on $R_t(XF)$. The calculated bond lengths agree with those observed for fluoride crystals by Shannon (1976) to within ~0.04Å.

Calculations on oxide, sulfide, and nitride molecules by Gibbs et al. (1987b), Bartelmehs et al. (1989) and Buterakos et al. (1992), respectively, have established correlations between bond length, R, and the bonding parameter, $p = s/r$ where s is the Pauling bond strength and r is the row number of the X cation. These studies also establish similar correlations between p and R calculated for chemically

Table 1. Observed and theoretical bond lengths, $R_o(XF)$ and $R_t(XF)$, and crystal (Shannon, 1976), bonded, and promolecule radii, $r_c(X)$, $r_b(X)$, and $r_p(X)$, for the metal atom.

$H_{m-n}X^{n+}F_m$	XF	$R_o(XF)$	$R_t(XF)$	$r_c(X)$	$r_b(X)$	$r_p(X)$
H_3LiF_4	LiF	1.88	1.81	0.73	0.70	0.72
H_5LiF_6	LiF	2.05	1.96	0.90	0.75	0.77
$HBeF_3$	BeF	1.45	1.46	0.30	0.52	0.53
H_2BeF_4	BeF	1.56	1.54	0.41	0.54	0.55
H_4BeF_6	BeF	1.74[1]	1.73	0.59[1]	0.60	0.61
BF_3	BF	1.30	1.30	0.15	0.44	0.45
HBF_4	BF	1.40	1.39	0.25	0.46	0.47
H_3BF_6	BF	1.56[1]	1.59	0.41[1]	0.52	0.57
CF_4	CF	1.44[2]	1.30	0.29[2]	0.42	0.49
H_2CF_6	CF	1.45[3]	1.52	0.30[3]	0.56	0.67
HNF_6	NF	1.42[3]	1.50	0.27[3]	0.69	0.72
H_3NaF_4	NaF	2.28	2.13	1.13	0.99	1.01
H_4NaF_5	NaF	2.29	2.18	1.14	1.00	1.03
H_5NaF_6	NaF	2.31	2.22	1.16	1.02	1.04
H_2MgF_4	MgF	1.86	1.85	0.71	0.83	0.85
H_3MgF_5	MgF	1.95	1.92	0.80	0.86	0.87
H_4MgF_6	MgF	2.01	1.96	0.86	0.87	0.89
$HAlF_4$	AlF	1.68	1.68	0.53	0.73	0.75
H_2AlF_5	AlF	1.77	1.75	0.62	0.75	0.77
H_3AlF_6	AlF	1.82	1.80	0.675	0.77	0.79
SiF_4	SiF	1.55	1.56	0.40	0.65	0.68
H_2SiF_6	SiF	1.69	1.68	0.54	0.69	0.72
PF_5	PF	1.58	1.55	0.43	0.62	0.65
HPF_6	PF	1.67[1]	1.61	0.52[1]	0.64	0.68
SF_6	SF	1.58[1]	1.55	0.43[1]	0.60	0.68

[1] Denotes radii calculated from bond length–bond strength curves
[2] Denotes radii from Pauling
[3] Denotes radii from Ahrens

similar molecules. In an examination of how p relates to $R_o(XF)$, $\ln[R_o(XF)]$ was plotted against $\ln(p)$ (Fig. 2a). A linear regression analysis of the data set shows that more than 98% of the variation of $\ln[R_o(X)]$ can be explained in terms of a linear dependence on $\ln(p)$. Using the estimates of the slope and intercept of the line, the expression $R(XF) = 1.34p^{-0.22}$ can be derived which reproduces the observed bond lengths to within ~ 0.06Å. Similarly, p correlates with the bond length data, $R_t(XF)$, obtained in MO calculations on fluoride molecules containing first and second row
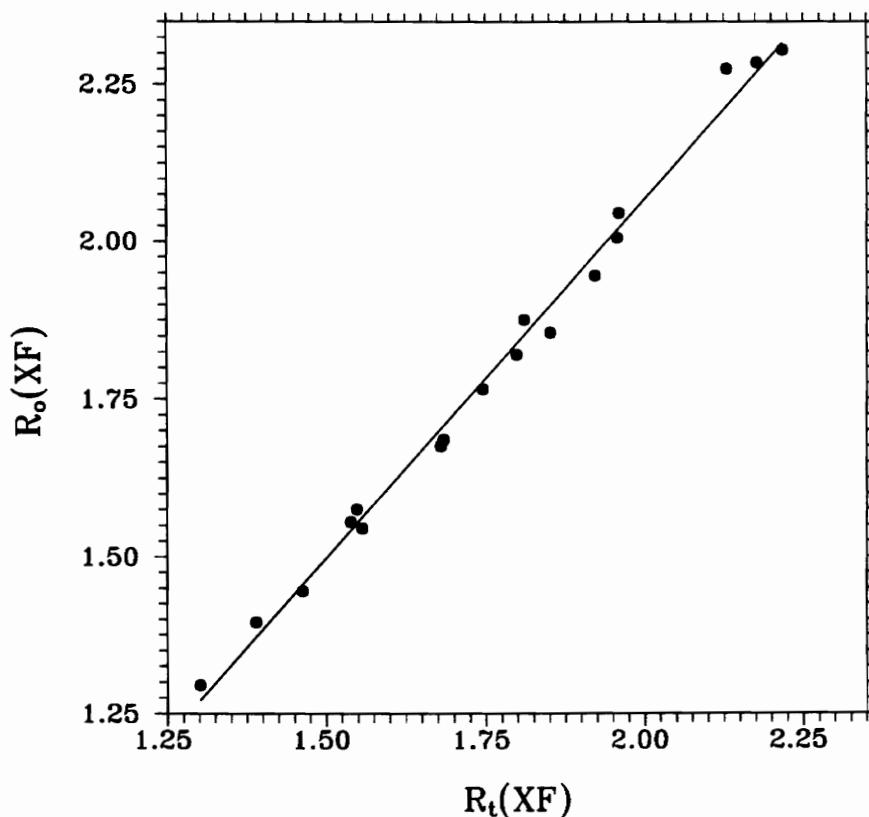
Figure 1. A scatter diagram of average XF bond length, $R_o(XF)$, where X is a row 1 or 2 main group cation, plotted against the theoretical XF bond length, $R_t(XF)$, calculated from molecular orbital methods. The $R_t(XF)$ match the $R_o(XF)$ to within ~ 0.04Å.

cations. A scatter diagram of $\ln[R_t(XF)]$ vs. $\ln(p)$ is displayed in Figure 2b. A linear regression of this data yields an R^2 value of 99.0 and the expression $R(XF)=1.33p^{-0.22}$ which also reproduces the theoretical bond lengths to within ~ 0.06Å. These two formulas relating observed and theoretical bond length data for crystals and molecules, respectively, are statistically identical, indicating that the forces that govern bond length variations in fluoride molecules and crystals can be viewed as similar. Furthermore, the exponent derived for the fluorides (-0.22) is statistically identical with those derived for oxides (-0.22), sulfides (-0.21), and nitrides (-0.22). As these values are statistically identical, a $p = -0.22(\approx \frac{-2}{9})$ is accepted for each of these

5

materials. These results indicate that for a given p–value, the relative change of a bond length in a nitride, oxide, fluoride and sulfide molecule or crystal relative to p is virtually the same (Gibbs and Boisen, 1986).
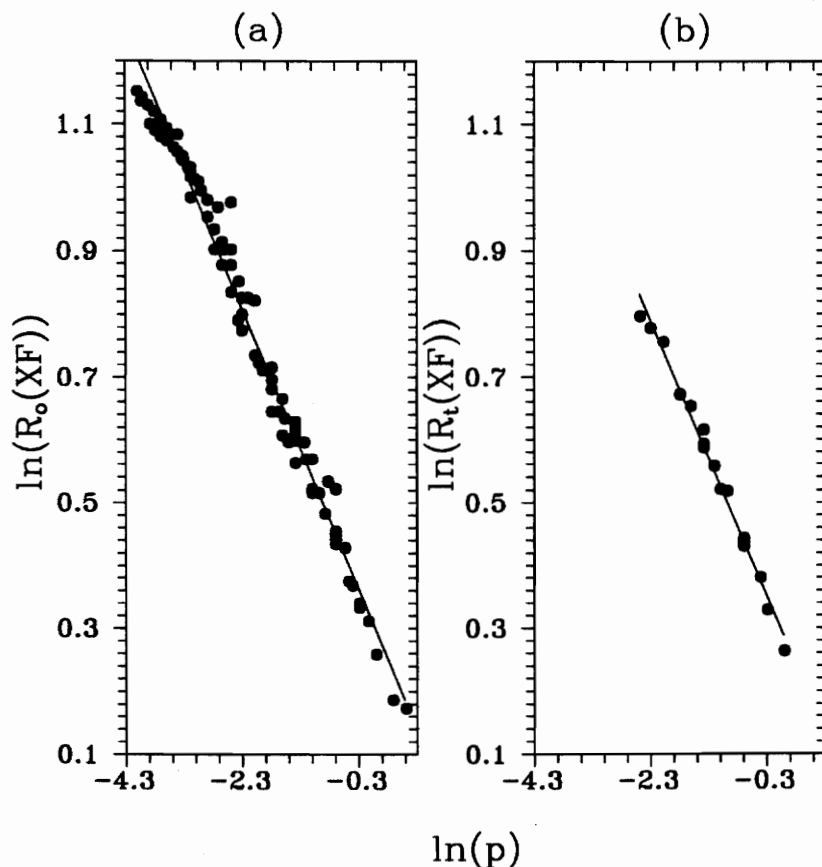
Figure 2(a-b). Scatter diagrams plotting the natural log of the XF bond length against the natural log of the bonding parameter, p. (2a) $\ln[R_o(\mathrm{XF})]$ and (2b) $\ln[R_t(\mathrm{XF})]$ plotted against $\ln(p)$. The slopes of these curves are statistically identical and yield the equation $R(\mathrm{XF})=1.34p^{-0.22}$. This equation produces XF bond lengths that match observed XF bond lengths to within ~ 0.06Å, on average.

One question that remains is whether the bond lengths for oxide, nitride, fluoride and sulfide molecules with non–main group metal cations also match those observed for crystals. To answer this question, the bond lengths for more than 170 molecules were plotted against those observed for crystals (Fig. 3). Those observed for molecules with transition metal cations agree with those observed for crystals to

6
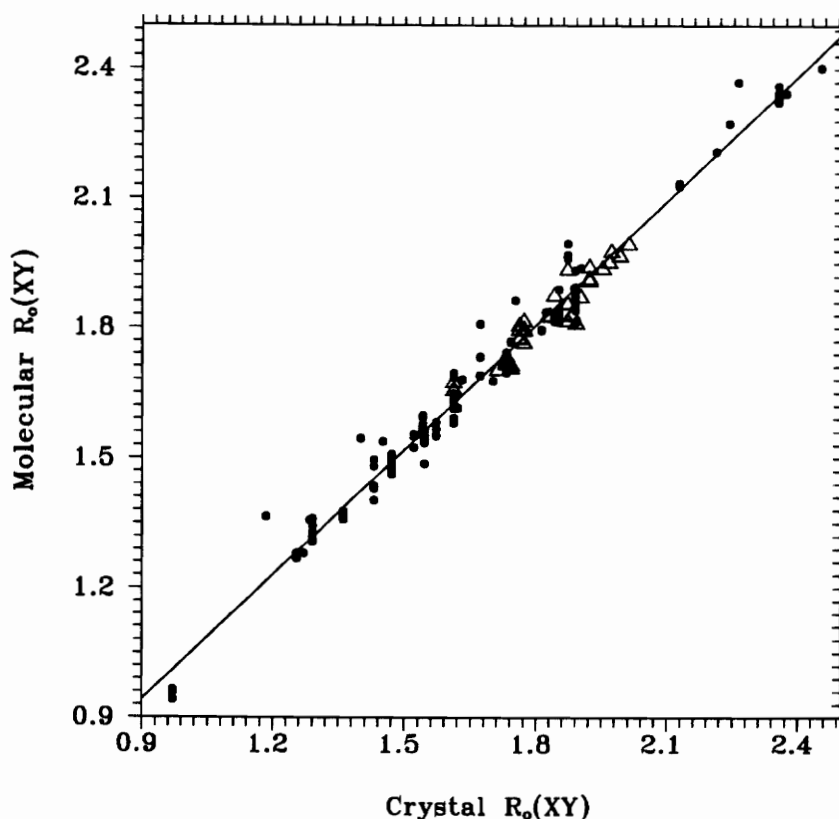
Figure 3. Scatter diagrams plotting observed XF bond lengths in molecules against XY bond lengths observed in crystals, where X is a main group or transition metal atom and Y is O, S, N, F, Se, and others. Data containing main group metal atoms are plotted as small solid circles while those containing transition metal atoms are plotted as open triangles. Note that bonds containing transition metal atoms seem to correlate about as well as those containing main group cations.

within ~ 0.03Å, whereas those recorded for molecules with main group metal cations agree to within ~ 0.04Å. The bond length data used to prepare the plot were observed for free polyatomic molecules that comprise a wide range of chemically different main and non–main group metal containing oxide, sulfide, fluoride, nitride and selenide coordinated polyhedra (Landolt–Boïnstein, 1976; 1987). Clearly, the agreement between the two data sets is equally good, regardless of the type of cation that is bonded to an anion. This agreement explains in part why Slater (1964) was successful in deriving a universal set of atomic radii that reproduces bond lengths observed for more

7

than 1200 molecules and chemically similar ionic, covalent, intermetallic and metallic crystals with an average deviation of 0.12Å. These radii were found to hold for covalently, metallically and ionically bonded materials equally well and to correlate remarkably well with the radial charge densities of the outermost shells of the atoms. However, the reproduction of bond length data with Slater's (1964) atomic radii is less precise than that of the Shannon (1976) radii because no attempt was made by Slater to correct his radii for such factors as coordination number, oxidation number and spin state.

Chapter 2
BONDED AND PROMOLECULE RADII
Introduction

Ever since Bragg (1920) first proposed that the bond lengths of crystals can be estimated by summing the radii of the two atoms comprising a bond, successively more elaborate sets of radii have been derived and used (1) to predict bond lengths, (2) to predict whether one atom in a crystal can be replaced by another, (3) to rationalize structural types in terms of structural field maps and (4) to serve as a basis for correlating and rationalizing structural and physical properties (For a good history of radii, see Pauling, 1960; Slater, 1965; Shannon and Prewitt, 1969; Shannon, 1976). Despite the considerable success that modern crystal (and ionic) radii have had in reproducing the average bond length for a given coordinated polyhedron, such radii are not in general realistic indicators of the true sizes of ions, particularly as they relate to the electron distribution of the bonded atoms in either a molecule or a crystal (Shannon and Prewitt, 1969; Gibbs et al., 1992). Gourary and Adrian (1960) and Slater (1965) have argued that a set of more realistic radii referred to as bonded radii by Bader et al., (1971) can be derived from the electron density distribution of either a molecule or crystal by measuring the distance along the bond path between the nuclei of a pair of bonded atoms and the point of minimum electron density along the bond path. As the electrons and nuclei of the atoms of a bonded system strive to adopt an arrangement wherein the total energy of the resulting configuration is minimized, the bonded radius, r_b, of an atom in the direction of a given bond can be regarded as a minimum energy feature. In the promolecule model, the positions of the nuclei are fixed and the total electron density distribution is simply a superposition of spherically averaged electron density distributions of atoms. Like the bonded radius,

9

the promolecule radius, r_p, of an atom is determined by measuring the distance between the nucleus and the point of minimum electron density along the bond path.

As observed in this study and elsewhere (Gibbs et al., 1992), bonded (and promolecule) radii differ from crystal (and ionic) radii in several important ways: (1) Each cation and anion typically has several different bonded (or promolecule) radii, a different one in the direction of each of its nonequivalent bonds while they each have a single crystal radius for a given chemical environment and condition and (2) Cations and anions each have a given crystal radius for a given coordination number, all other things being equal (such as valence, spin state, etc.), whereas for a given coordination number, bonded (and promolecule) radii increase in a regular way with bond length.

Bonded radii are determined from the total electron density maps of the molecules to learn whether the radius of the fluoride ion varies in a regular way with bond length as observed for the nitride, oxide and sulfide ions. Radii observed for the atoms in rock salt, bromellite and several silicates will be compared with theoretical bonded radii generated with molecular orbital methods and promolecule radii calculated for the coordinated polyhedra of these minerals.

Systematics of Bonded and Promolecule Radii Variations

In accordance with the above observation (2), the bonded radius of the 6-coordinate chloride ion in rock salt is observed to increase from 1.64Å for a bond length $R(NaCl) = 2.82$Å to 1.70Å in sylvite with $R(KCl) = 3.15$Å while the ionic radius of the chloride ion is assumed to be constant (1.81Å) and independent of bond length (Slater, 1965). Similarly, the bonded radius of the 2-coordinate oxide ion in coesite is observed to increase from 0.92Å to 0.97Å for SiO bond lengths of 1.595Å and 1.621Å respectively, while the crystal radius of the oxide ion is assumed to be

constant (1.21Å) and independent of bond length (Gibbs et al., 1992). In addition, sets of bonded radii calculated from electron density distributions for a large number of minimum energy oxide, sulfide and nitride molecules show that the bonded radii of the anions in these molecules increase in a regular way with bond length. In these calculations, sets of bonded radii for first and second row main group cations were obtained (Gibbs and Boisen, 1986; Bartelmehs et al. 1989; Buterakos et al. 1992). In all cases, it was observed that the bonded radii of the anions, $r_b(Y)$, where Y is O, S, or N increase in a regular manner with increasing bond length, $R_t(XY)$. It was also observed that the radii of the anions decrease with the row number, r, of the main group cation, X, to which it is bonded. From these relationships the following expressions were derived:

$$r_b(O) = (0.35 - 0.10r) + 1/2R_t(XO),$$

$$r_b(N) = (0.38 - 0.12r) + 1/2R_t(XN),$$

$$r_b(S) = (0.59 - 0.13r) + 1/2R_t(XS).$$

The coefficient of 1/2 for $R_t(XY)$ is interpreted as indicating that the variation in bond length is shared equally between the bonded radius of the cation and the anion.

In an examination of whether the bonded radius of the fluoride ion varies in a similar way, electron density maps (see Appendix B) were calculated for 25 $H_{m-n}X^{n+}F_m$ fluoride molecules containing 3−, 4−, 5−, and 6− coordinated first and second row main group cations, X. The calculations were completed using a FORTRAN77 program entitled EDEN and the density matrices provided by GAUSSIAN86 Roothaan-Hartree-Fock SCF single-point calculations at the minimum energy molecular geometries. In the determination of the bonded radii, it is assumed that the radius of the atom in the direction of a neighboring atom is the distance from the center of the atom

to the point of minimum electron density along the line connecting the two atoms. The minimum was located analytically using a strategy based on the quasi–Newton method (Gibbs et al, 1992) in which a quartic polynomial was fit to the data. The resulting radii for the fluoride ion, $r_b(F)$ (Table 1), are plotted against $R_t(XF)$ in Figure 4. A regression analysis of $r_b(F)$ against $R_t(XF)$ yields the following expression:

$$r_b(F) = (0.40 - 0.07r) + 1/2R_t(XF).$$

This equation is similar to that derived for the oxide, sulfide and nitride molecules and suggests that variation in XF bond length is shared, as observed for the oxide, nitride and the sulfide anions, equally by the bonded radius of the anion and the cation.

A comparison of the bonded radii for the oxide, fluoride, nitride and sulfide molecules shows that the radius of a given cation X in a sulfide molecule is, on average, ~ 0.1Å larger than it is in either an oxide or a fluoride molecule and ~ 0.05Å larger than it is in a nitride molecule. An examination of the minimum energy bond lengths for these molecules shows, for a given X–cation, that $R(XS)$ is slightly longer than $R(XN)$ which in turn is slightly longer than $R(XO)$ and $R(XF)$. In other words, an X cation is larger when it is bonded to sulfur (longer bond), it has an intermediate value when bonded to nitrogen and it is smallest when bonded to either oxygen or fluorine (shorter bonds).

Modern crystal and ionic radii such as those derived for the oxides and fluorides reproduce average bond lengths for coordinated polyhedra with a precision of ~ 0.02Å when coordination number, spin state, and oxidation state are taken into account (Shannon and Prewitt, 1969; Shannon, 1976). Despite the fact that these radii are relative, they correlate well with the bonded radii for the cations calculated for the oxide molecules (Gibbs and Boisen, 1986) and the fluoride molecules studied
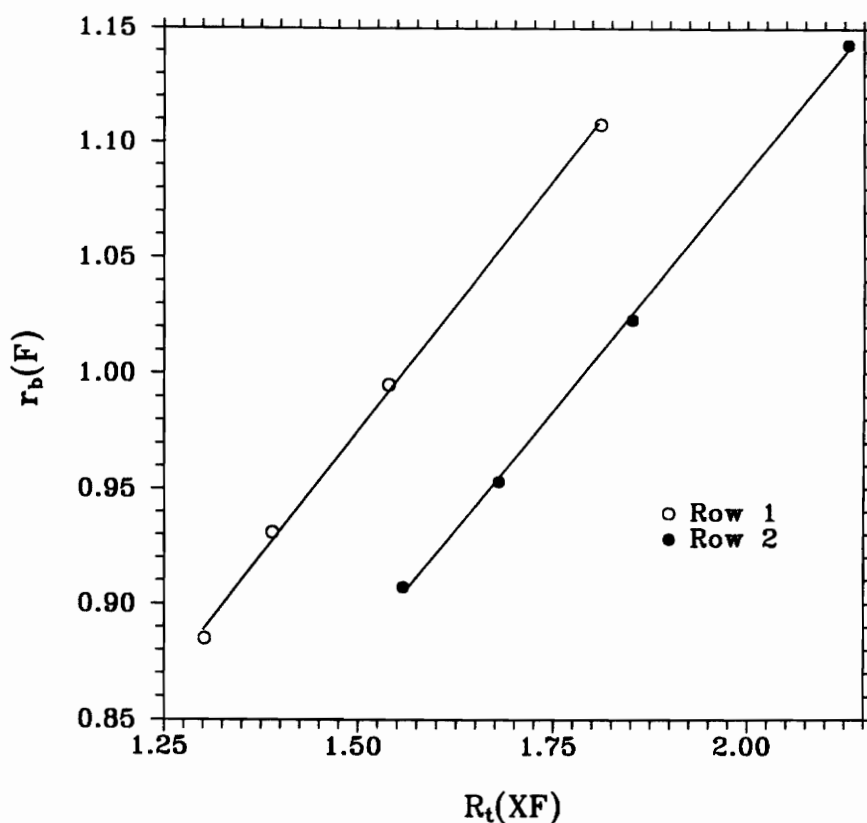
Figure 4. Scatter diagrams plotting the bonded radius of the fluorine anion, $r_b(F)$, when bonded to tetrahedrally coordinated row 1 and 2 main group metal atoms. The open circles represent data from row 1 and the solid circles represent data from row 2.

here. Similarly, the crystal radii derived for sulfides correlate equally well with the bonded radii calculated for sulfide molecules (Bartelmehs et al., 1989). In addition, Cahen (1988) has found that averaged bonded radii derived from plots of total valence electron densities also correlate with sulfide crystal radii. He also made the important observation that a model based on such bonded radii provides a better understanding of the ease with which Cu can be leached from the enargite Cu_3AsS_4 structure than can be provided by a model based on either ionic or crystal radii.

Not only do crystal radii correlate well with bonded radii, but Feth et al. (1993) found that they correlate equal well with promolecule radii. In the above study,

13

promolecule electron density distributions were calculated for ideal tetrahedral and octahedral coordinated polyhedra containing main group and non−main group cations from the first four rows of the periodic table with bond lengths set equal to the crystal radius sum of the cation and anion. The high correlations that obtain between the resulting promolecule radii and the crystal radii for oxides and sulfides and the ionic radii for nitrides shows that Shannon and Prewitt (1969), Shannon (1976) and Shannon (1981) did an excellent job ordering their radii one relative to another as did Baur (1987) in ordering his nitride ionic radii.

In the formation of a crystal like rock salt, the assertion is often made that Na loses an electron to become Na^+ while Cl gains the electron to become Cl^-. With this exchange of electrons, it is generally accepted that the resulting Cl^- anion is significantly larger than the Cl atom. With the loss of an electron, the resulting Na^+ cation is assumed to be smaller than the atom with the separation between the two atoms remaining essentially unchanged. On the other hand, Slater (1965) has concluded from valence shell orbital overlap considerations and a covalent model that the atoms in an alkali halide like rock salt are more nearly neutral than a fully ionic model would indicate. He continued by concluding that it would be likely that the difference in a total electron density distribution generated by the superposition of atomic electron densities and one generated by the superposition of ionic densities would be small and subtle. Moreover, he believed that it would be very difficult to distinguish one from the other by examining the resulting electron density map. In other words, the electron density distribution of a typical ionic material like rock salt would appear to have a large amount of atomic character.

In an examination of the experimental electron density maps recorded for rock salt, Witte and Wölfel (1955) reported bonded radii of 1.17Å for Na^+ and 1.64Å
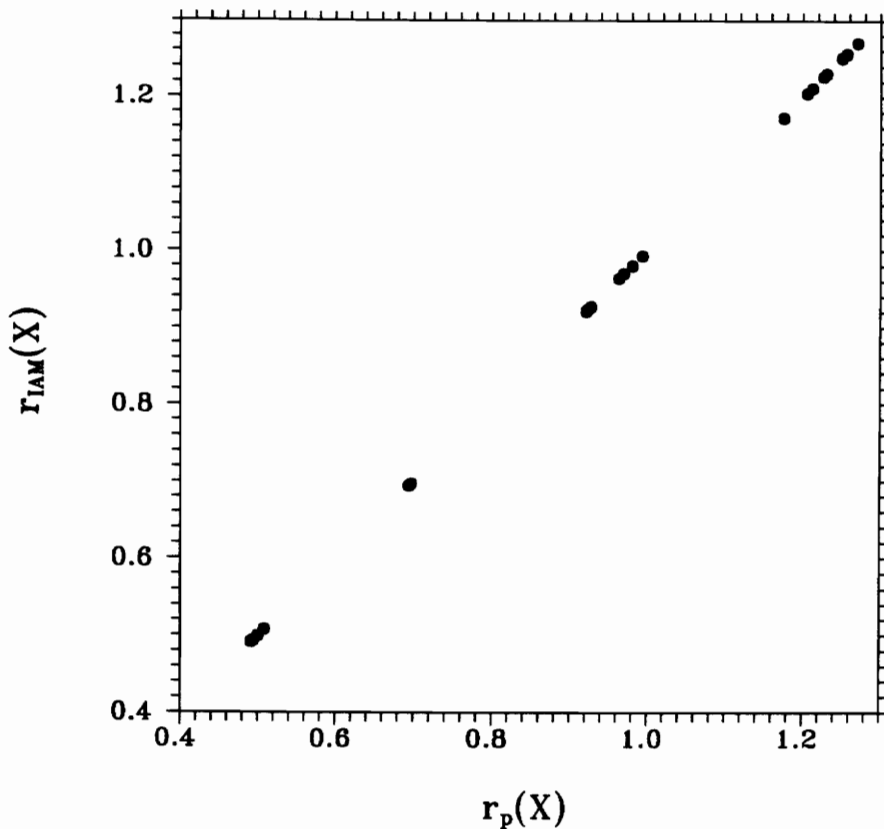
Figure 5. Scatter diagrams plotting the independent atom model (IAM) procrystal radii against the promolecule radii derived from calculations on only the coordinated polyhedra in danburite. Structural data for danburite was obtained from Downs (1992).

for Cl^-. A generation of the total electron density for a small $Na_{13}Cl_{14}$ block of the rock salt structure, assuming the superposition of spherically averaged atomic distributions of Na and Cl yield promolecule radii, r_p, for Na and Cl of 1.166Å and 1.654Å, respectively. The promolecule electron density distribution of rock salt decays rapidly with distance from the nucleus of each atom such that the density is less than 0.01 e/bohr^3 at a distance of only ~ 1.6Å(Gibbs et al., 1992). Because of this rapid drop in density, the promolecule radii for Na and Cl calculated for a separation of 2.82Å(the NaCl separation in rock salt) were found to be largely independent of coordination number of the Na atom with $r_p(^{II}Na) = 1.168$Å in a $NaCl_2$ molecule

15

and $r_p(^{VI}\text{Na}) = 1.165\text{Å}$ in a NaCl_6 coordinated polyhedron.

Promolecule electron density maps calculated for the BeO_4, SiO_4, CaO_7, SiO_6 coordinated polyhedra observed for bromellite, danburite and stishovite yield promolecule radii for Be, Si, Ca and O that match the bonded radii obtained from experimental electron density maps to within 0.01Å (Feth et al., 1993). In addition, procrystal IAM radii obtained for the atoms in danburite (Downs, 1992) agree to withinff 0.002Å with promolecule radii calculated for the atoms comprising the coordinated polyhedra of the mineral (Fig. 5). A procrystal is a model of a crystal whose electron density distribution, like that of a promolecule, consists of a superposition of spherically averaged electron density distribution of atoms, each located at its observed position in the crystal. Procrystal radii are obtained in the same way that promolecule radii are determined for such a distribution. Collectively, when considered with the agreement that obtains between the bonded and promolecule radii for rock salt, these results support arguments by Slater (1965) that the electron density distributions in such crystals can be viewed as having a relatively large atomic component, regardless of bond type. It also indicates that promolecule radii calculated for the atoms of a coordinated polyhedron isolated from a crystal closely match procrystal radii calculated for the crystal. This result suggests, as argued for the Na and Cl atoms in rock salt, that the electron density of the atoms in danburite decay rapidly with distance. Gibbs et al. (1992) also observed that promolecule radii calculated for the oxide, nitride and sulfide molecules optimized by Gibbs et al. (1987b), Buterakos et al. (1992) and Bartelmehs et al. (1989), respectively, yield promolecule radii that are highly correlated with the bonded radii calculated for the atoms in these same molecules (data plotted as open circles in Fig. 6). To learn whether the bonded radii calculated for the fluoride molecules show a similar correlation, promolecule radii

were calculated for the X–cations comprising the fluoride molecules. The resulting promolecule radii are plotted as solid circles in Figure 6 against the bonded radii of the X–atoms calculated for the fluoride molecules. The resulting radii match those obtained for the oxide, nitride and sulfide molecules reasonably well. It is noteworthy that the fluoride data fall closer, on average, to the line than the remaining data, a result that probably reflects the fact that the radii for the fluorides were determined analytically whereas those obtained for the oxides, sulfides and nitrides were obtained using graphical methods. Nonetheless, the strong correlation that obtains between the bonded and promolecule radii indicates, as observed above, that the electron density distributions of the molecules used to prepare the plot can be viewed as having either large atomic components or the property that atoms and their ions possess similar bonded radii.

Bond Length and Radii Variations in Silicates

A similar study of experimental electron density distributions indicates that the bonded radii of Si and O in several silicates are independent of coordination number for a given bond length but increase with SiO bond length as observed for the cations in the rock salt structure. In this study, the bonded radii for ^{IV}Si and ^{II}O were calculated for the monosilicic acid molecule, H_4SiO_4, for a range of SiO bond lengths from 1.50Å to 1.80Å and compared with those obtained from experimental electron density maps determined for two silicate crystals (coesite and danburite) that have 4–coordinate Si and 2–coordinate O and one (stishovite) that has 6–coordinate Si and 3–coordinate O. If the radii are independent of coordination number for a given bond length, then the bonded radii calculated for the silicate molecule are expected to match those observed for the three crystals.

For the calculation, the geometry of H_4SiO_4 was optimized assuming S_4 point
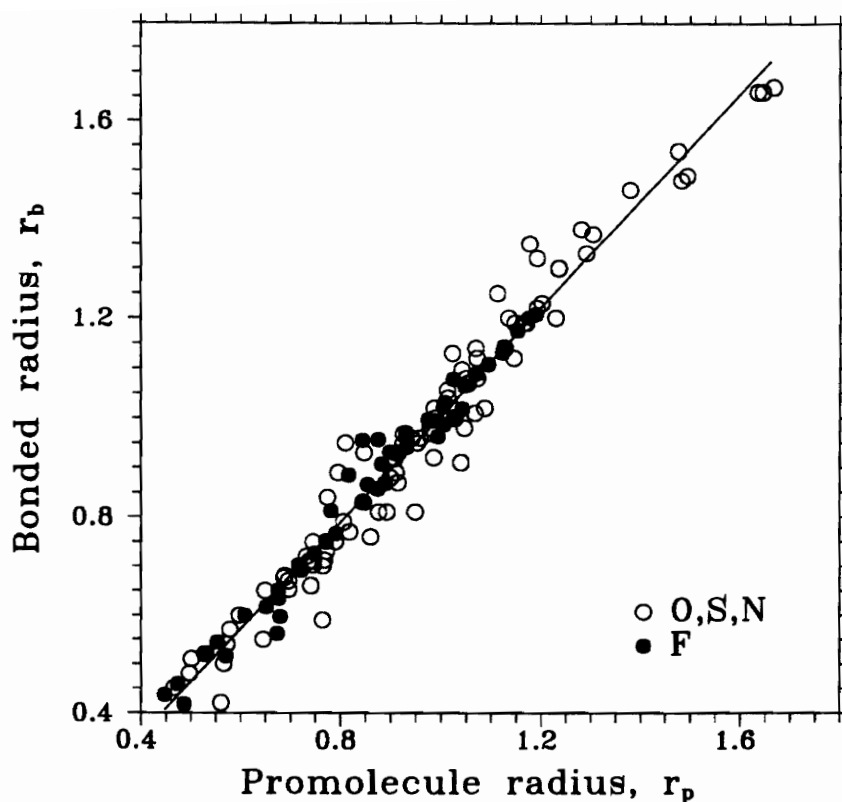
Figure 6. Plot of the bonded radii of the main group cations and anions versus promolecule radii derived from calculations on oxide, sulfide, nitride and fluoride molecules. Data for the oxides, sulfides and nitrides are plotted as open circles while data for the fluorides are plotted as solid ones.

symmetry and a 6–31G** basis set (Gibbs et al., 1981; Boisen and Gibbs, 1986). Additional SCF calculations were completed for the resulting molecule with the SiO bond length set at a range of values that include those reported for the three silicate crystals. Using the density matrices provided by each calculation and the software EDEN, bonded radii for both Si and O were calculated for each molecule. The resulting radii vary linearly with $R(\mathrm{SiO})$ as evinced by Figure 7 with $r_b(\mathrm{O})$ increasing with $R(\mathrm{SiO})$ about three times more rapidly than $r_b(\mathrm{Si})$. The bonded radii provided by the structural analyses of the three silicate crystals are plotted in Figure 7 as solid circles. Those determined by the mapping of the experimental electron density

18

distribution of stishovite fall on the curve while those determined for the silicate tetrahedra in coesite and danburite scatter about the curve departing at most by ~0.02Å. The agreement between the bonded radii calculated for the molecule and those obtained experimentally provide support for the assertion that the electron density distribution in molecules like H_4SiO_4 and $H_6Si_2O_7$ are similar to those in a silicate crystal.

Discussion

Molecular orbital calculations completed on molecular models of blocks of crystals have provided evidence that the forces that govern bond lengths can be viewed as if largely short ranged. This viewpoint is almost certainly true, otherwise, it would be unlikely that one could derive single sets of radii that would generate the average bond lengths for the coordinated polyhedra for a wide variety of oxide, nitride, fluoride and sulfide crystals to within ~0.02Å, based only on such parameters as coordination number, spin state, and oxidation state. Because such sets of radii do indeed exist, the separation between a pair of bonded atoms in such crystals can be viewed as largely independent of any other forces exerted on the pair by the other parts of the structure. Because of the short ranged character of these forces, a knowledge of the wave functions and the charge density distribution of a molecule, provided by molecular orbital calculations, can improve our understanding of such properties for representative parts of a chemically similar crystal. By completing such calculations, the results can be transferred to the crystal and used to improve our understanding of its crystal chemistry.

As observed by O'Keeffe and Hyde (1985) at The Castle Hot Springs Conference on Structure and Bonding, the divorce between crystal chemistry and molecular chemistry in the early thirties was a mistake in that it left both sciences the poorer.
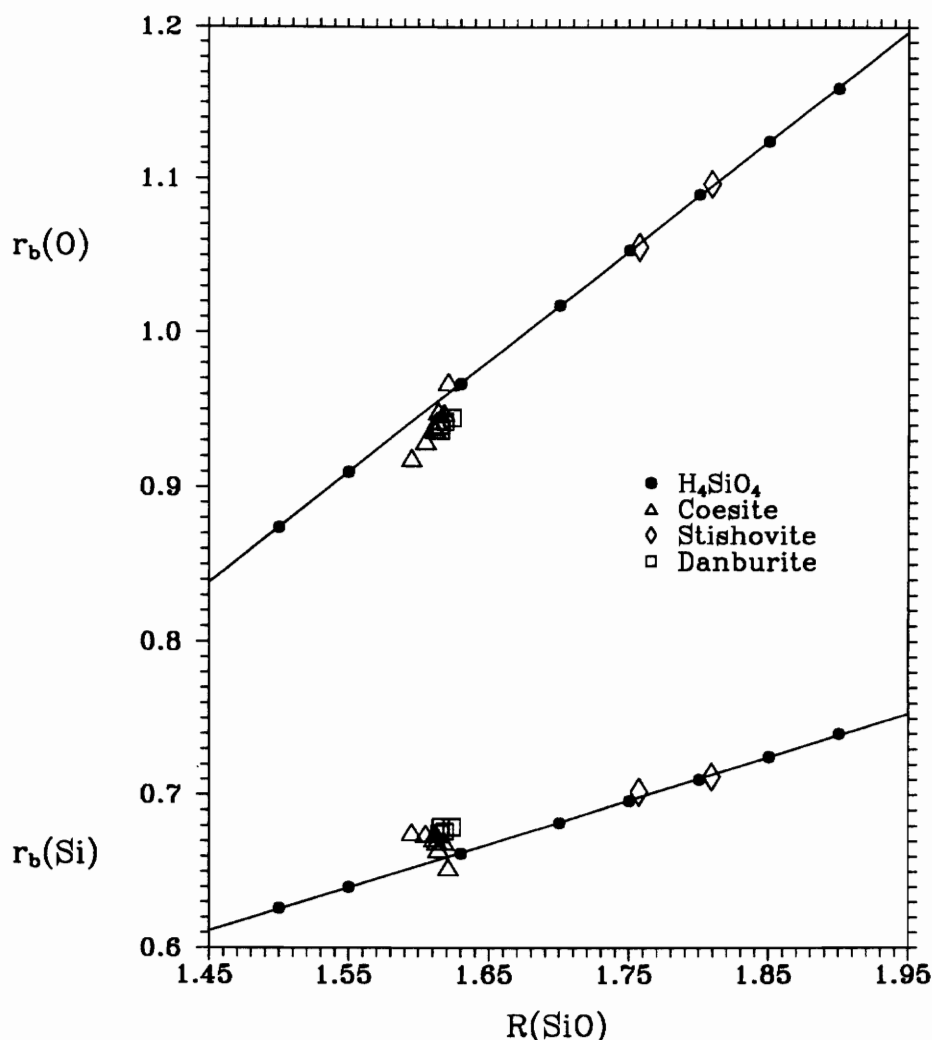
Figure 7. Scatter plots of the bonded radii of Si and O, $r_b(Si)$ and $r_b(O)$ respectively, in monosilicic acid, H_4SiO_4 versus SiO bond lengths, $R(SiO)$ over a range from 1.50Åto 1.90Å. These data are plotted as solid circles. Also plotted on these diagrams are the bonded radii of Si and O for coesite (open triangles), stishovite (open diamonds) and danburite (open squares). Notice how well data from stishovite falls on the plot, though stishovite has 6–coordinated Si and 3–coordinated O. Data for coesite and stishovite were obtained from Buterakos (1990) and data for danburite were obtained from Downs and Swope (1992).

The insights provided into bond length and angle variations and charge density distributions calculated for molecules with molecular orbital methods and the successful transference of the results to crystals provides support for the statement that the structures of molecules, their properties and their similarities with crystals should be included as a chapter in any course on crystal chemistry. In addition, in studies

using molecules as models for bonding in silicates, molecular orbital methods have been used to probe and clarify the similarities of the binding forces in molecules and chemically similar coordination polyhedra in silicate crystals. There is no doubt that the results of these studies have improved our understanding of silicate crystal chemistry. As discussed in the introduction, the methods have not only generated the bond length and angle variations exhibited by crystals, but they have also provided a theoretical underpinnings for a number of empirically established correlations. The methods also show that calculations for a large number of oxide, nitride and sulfide molecules yield bond lengths that match those observed in chemically similar crystals. In addition, the calculations undertaken in this study show that the bond lengths in fluoride molecules match those in crystals as well. They also show that the bonded radii of the cations and the fluoride ion in these molecules increase in a regular way with both length. It is also observed that bonded radii can be easily derived from electron density distributions calculated for molecules. However, unlike ionic and crystal radii, bonded radii seem to depend both on the atom to which they are bonded and the length of the bond. For a given bond length, they also seem to be independent of their coordination numbers. Also, individual atoms are observed to exhibit several different radii, depending on their chemical environments, rather than a single radius.

For example, the oxide ions in danburite each exhibit several different bonded radii that range between ~ 0.94 and ~ 1.23Å (Downs and Swope, 1992). Three of the oxide ions are bonded to three different cations, ^{IV}B, ^{IV}Si and ^{VII}Ca at ~ 1.47, ~ 1.62 and ~ 2.44Å, respectively. In the direction of the BO bonds, the oxide ions exhibits a radius of ~ 1.00Å, in the direction of the SiO bonds, a radius of ~ 0.94Å while in the direction of the CaO bonds, a radius 1.23Å. Of the two remaining nonequivalent

oxide ions, one is bonded to two equivalent ^{IV}B atoms and a ^{VII}Ca atom and has a radius of 1.18Å in the direction of the CaO bond and a radius of 0.97Å in the direction of the two BO bonds. The remaining oxide ion is bonded to two equivalent ^{IV}Si atoms and exhibits a single radius of 0.94Å. The cations in danburite also show variable radii but the variability is much smaller. In the derivation of ionic and crystal radii, it is assumed that such radii are spherical. However, the results presented here indicate that electron density distributions measured for an atom in the directions of nonequivalent bonds are aspherical and yield several different radii rather than a single one. This result and those presented above confirm proposals made by Johnson (1973), O'Keeffe (1981), Cahen (1988) and Gibbs et al. (1992) that cations and anions in molecules and crystals have variable radii rather than a single radius for a given chemical environment.

Finally, an examination of the total electron density distribution observed for danburite indicates that its CaO bonds have a large component of ionic structure which is consistent with bonds involving Ca^{2+} cations (Downs and Swope, 1992). If, as is generally believed, that Ca^{2+} cations are indeed smaller than Ca atoms, then the promolecule radii calculated for the Ca atom of a CaO_7 coordinated polyhedra and the procrystal (IAM) radii calculated for danburite should be larger than the observed bonded radii. But, as noted above, the bonded and the promolecule radii for the Ca atom in danburite agree with one another to within ~0.01Å, a result that indicates that the radius of an atom changes little, for a given bond length, upon a losing its valence electrons in forming a cation. The close agreement between bonded and promolecule radii is not restricted to the Ca atom in danburite, but it also obtains for the atoms in a wide variety of molecules and crystals with a wide range of bond types. On the basis of these results, it is evident that the bonded radius of an atom

remains unchanged with a loss of its electrons for a given bond length. Results such as these that involve a synthesis of experimental and calculated data for molecules and crystals surely enrich our understanding of the properties of ions, their sizes and size variations with bond length for molecules and crystals as well as enrich our understanding of the crystal chemistry of a solid state material that contains such ions.

REFERENCES

Bader, R.F.W., Beddall P.M., and Cade P.E. (1971) Partitioning and characterization of molecular charge distributions. Journal of the American Chemical Society, 93, 3095-3107.

Bartelmehs, K.L., Gibbs, G.V., and Boisen Jr., M.B. (1989) Bond-length and bonded-radii variations in sulfide molecules and crystals containing main-group cations: A comparison with oxides. American Mineralogist, 74, 620-626.

Baur (1970) Bond length variation and distorted coordination polyhedra in inorganic crystals. Transactions of the American Crystallographic Association, 6, 129-155.

Baur, W.H. (1987) Effective ionic radii in nitrides. Chemical Reviews, 1, 59-83.

Boisen, M.B., Jr., Gibbs, G.V., Downs, R.T. and D'Arco, P. (1990) The dependence of the SiO bond length on structural parameters in coesite, the silica polymorphs and the clathrasils. American Mineralogist, 75, 748-754.

Boisen, M.B., Jr. and Gibbs, G.V. (1993) A modeling of the structure and compressibility of quartz with a molecular potential and its transferability to cristobalite and coesite. , , in press.

Bragg, W.L. (1920) The arrangement of atoms in crystals. Philosophical Magazine and Journal of Science, 40, 169-189.

Brown, G.E., Gibbs, G.V., and Ribbe, P.H. (1969) The nature and variation in length of the Si-O and Al-O bonds in framework silicates. American Mineralogist, 54, 1044-1061.

Brown, I.D. and Shannon, R.D. (1973) Empirical bond-strength–bond-length curves for oxides. Acta Crystallographica, A29, 266-282.

Buterakos, L.A. (1990) Bond length and bonded radii variations in nitride molecules and crystals. MS Dissertation. Virginia Polytechnic Institute and State University, 28 pp.. Blacksburg, Virginia.

Buterakos, L.A., Gibbs, G.V., and Boisen Jr, M.B. (1992) Bond length variation in hydronitride molecules and nitride crystals. Physics and Chemistry of Minerals, 19, 127-132.

Cahens, D. (1988) Atomic radii in ternary adamantines. Journal of Physics and Chemistry of Solids, 49(1), 103-111.

Chelikowsky, J.R., King, H.E., Jr., Troullier, N., Martins, J.L. and Glinnemann, J. (1990) Structural properties of α–quartz near the amorphous transition. Physical Review Letters, 65, 3309-3312.

Clementi, E., and Roetti, C. (1974) Atomic data and nuclear data tables: Roothaan-Hartree-Fock atomic wave functions. Academic Press, New York, NY.

Cruickshank, D.W.J. (1961) The role of 3d–orbitals in π–bonds between (a) silicon, phosphorous, sulfur, or chlorine and (b) oxygen or nitrogen. The Journal of the Chemical Society, 1077, 5486-5504.

Downs, J.W. (1992) personal communication. , , .

Downs, J.W. and Swope, R.J. (1992) The laplacian of the electron density and the electrostatic potential of danburite, $CaB_2Si_2O_8$. Journal of Physical Chemistry, 96, 4834-4840.

Feth, Shari, Gibbs, G.V., and Boisen, M.B., Jr. (1993) Promolecule and crystal radii correlations for nitrides, oxides, and sulfides. EOS, Abstract, Spring Meetings., 167.

Frisch, M.J., Binkley, J.S., Schlegel, H.B., Rahavachari, K., Melius, C.F., Martin, R.L., Stewart, J.J.P., Bobrowicz, F.W., Rohlfing, C.M., Kahn, L.R., Defrees, D.J., Seeger, R., Whiteside, R.A., Fox, D.J., Fleuder, E.M. and Pople, J.A. (1984) Gaussian 86. Carnegie-Mellon Quantum Chemistry Publishing Unit, Pittsburgh, PA.

Geisinger,K.L. and Gibbs, G.V. (1981) SiSSi and SiOSi bonds in molecules and solids: A comparison. Physics and Chemistry of Minerals, 7, 204-210.

Gibbs, G.V. (1982) Molecules as models for bonding in silicates. American Mineralogist, 67, 421-450.

Gibbs, G.V., and Boisen Jr, M.B. (1986) Molecular mimicry of structure and electron density distributions in minerals. Materials Research Society Symposium Proceedings, 73, 515-527.

Gibbs, G.V., Boisen Jr, M.B., Downs, R.T. and Lasaga, A.C. (1988) Mathematical modeling of the structures and bulk moduli of TX_2 quartz and cristobalite structure-types, T=C,Si,Ge and X=O,S. Materials Research Society Symposium Proceedings, 121, 155-165.

Gibbs, G.V., D'Arco, P. and Boisen Jr, M.B. (1987a) Molecular mimicry of the bond length and angle variations in germinate and thiogerminate crystals: a comparison with variations calculated for carbon-, silicon-, and Sn-containing oxide and sulfide molecules. Journal of Physical Chemistry, 91, 5347-5354.

Gibbs, G.V., Finger, L.W., and Boisen Jr, M.B. (1987b) Molecular mimicry of the bond length - bond strength variations in oxide crystals. Physics and Chemistry of Minerals, 14, 327-331.

Gibbs, G.V., Hamil, M.M., Louisnathan, S.J., Bartell, L.S. and Yow, H. (1972) Correlations between Si–O bond length, Si–O–Si angle and bond overlap populations calculated using extended Huckel molecular orbital theory. American Mineralogist, 57, 1578-1613.

Gibbs, G.V., Meagher, E.P., Newton, M.D. and Swanson, D.K. (1981) A comparison of experimental and theoretical bond length and angle variations for minerals, inorganic solids, and molecules.. In M.O'Keeffe and A. Navrotsky, Eds., Structure and Bonding in Crystals. 1, 195-225. Academic Press, New York, NY.

Gibbs, G.V., Spackmanm, M.A. and Boisen Jr, M.B. (1992) Bonded and promolecule radii for molecules and crystals. American Mineralogist, 77, 741-750.

Gourary, B.S., and Adrian, F.J. (1960) Wave functions for electron-excess color centers in alkali halide crystals. Solid State Physics, 10, 127-247.

Johnson, O. (1973) Ionic radii for spherical potential ions. I. Inorganic Chemistry, 12, 780-785.

Julian, M.M. and Gibbs, G.V. (1985) Bonding in silicon nitrides. Journal of Physical Chemistry, 89(25), 5476-5480.

Julian, M.M. and Gibbs, G.V. (1988) Modelling the configuration about the nitrogen atom in methyl- and silyl-substituted amines. Journal of Physical Chemistry, 92(6), 1444-1451.

Landolt–Bornstein (1976) Numerical Data and Functional Relationships in Science and Technology. Group II: Atomic and Molecular Physics. Vol. 7, Structure Data of Free Polyatomic Molecules. Springer-Verlag, Berlin.

Landolt–Bornstein (1987) Numerical Data and Functional Relationships in Science and Technology. Group II: Atomic and Molecular Physics. Vol. 15, Structure Data of Free Polyatomic Molecules. Springer-Verlag, Berlin.

Lasaga, A.C. and Gibbs, G.V. (1987) Application of quantum mechanical potential surfaces to mineral physics calculations. Physics and Chemistry of Minerals, 14, 107-117.

Lasaga, A.C. and Gibbs, G.V. (1988) Quantum mechanical potential surfaces and calculations on minerals and molecular clusters I: STO–3G and 6–31G* results. Physics and Chemistry of Minerals, 16, 29-41.

Lasaga, A.C. and Gibbs, G.V. (1991) Quantum mechanical Hartree-Fock surfaces and calculations on minerals II: 6–31G* results. Physics and Chemistry of Minerals, 17, 485-491.

Newton, M.D. and Gibbs, G.V. (1980) *Ab initio* calculated geometries and charge distributions for H_4SiO_4 and $H_6Si_2O_7$ compared with experimental values for silicates and siloxanes. Physics and Chemistry of Minerals, 6, 221-246.

O'Keeffe, M. (1981) Some aspects of the ionic model for crystals. M. O'Keeffe, and A. Navrotsky (Eds) Structure and bonding in crystals. Vol II, pp 299-322. Academic Press, Inc., New York, NY.

O'Keeffe, M., and Hyde, B.G. (1985) An alternative approach to non-molecular crystal structures with emphasis on arrangements of cations. Structure and Bonding. Vol. 61, 77-144. Springer-Verlag Berlin, Heidelberg.

Pauling, L. (1960) The Nature of the Chemical Bond, 3rd edition. Cornell University Press, Ithaca, Ney York.

Purton, J., Jones, R., Catlow, C.R.A. and Leslie, M. (1993) Ab initio potentials for the calculation of the dynamical and elastic properties of α–quartz. Physics and

Chemistry of Minerals, 19, 392-400.

Shannon, R.D. (1976) Revised effective ionic radii and systematic studies of inter-atomic distances in halides and chalcogenides. Acta Crystallographica, A32, 751-767.

Shannon, R.D. (1981) Bond distances in sulfides and a preliminary table of sulfide crystal radii. In: M. O'Keeffe, and A. Navrotsky (Eds) Structure and bonding in crystals. Vol II, pp 53-70. Academic Press, Inc., New York, NY.

Shannon, R.D., and Prewitt, C.T. (1969) Effective ionic radii in oxides and fluorides. Acta Crystallographica, B25, 925-946.

Slater, J.C. (1964) Atomic radii in crystals. Journal of Chemical Physics, 41, 3199-3204.

Slater, J.C. (1965) Quantum theory of molecules and solids. Vol 2: Symmetry and energy bands in crystals. McGraw-Hill, Inc., New York, NY.

Smith, J.V. (1953) Reexamination of the crystal structure of melilite. American Mineralogist, 38, 643-661.

Stixrude, L. and Bukowinski, M.S.T. (1988) Simple covalent potential models of te-trahedral SiO_2: Applications to α–quartz and coesite at pressure. Physics and Chemistry of Minerals, 16, 199-206.

Tossel, J.A. and Gibbs, G.V. (1978) The use of molecular-orbital calculations on model systems for the prediction of bridging-bond-angle variations in siloxanes, silicates, silicon nitrides and silicon sulfides. Acta Crystallographica, A34, 463-472.

Tsuneyuki, S., Tsukada, M., Aoki, H. and Matsui, Y. (1988) First-principles inter-atomic potential of silica applied to molecular dynamics. Physical Review Letters, 61, 869-872.

Witte, H., and Wölfel, E. (1955) Röntgenographische bestimmung der elektronen-verteilung in kristallen: Die elektronenverteilung im steinsalz. Zeitschrift für Physikalische Chemie, Neue Folge, 3, 296-329.

Appendix A
REVIEW OF ELECTRON DENSITIES
Introduction

The purpose of this appendix is to outline a procedure by which total electron density maps, and details of their features, can be calculated for molecules. As the total electron density distribution, $\rho(\mathbf{r})$, of a molecule with an optimized geometry is a minimum energy feature, that is, it represents a ground state electron density distribution, features of $\rho(\mathbf{r})$, such as the (3,-1) critical points (cp's) and the bonded radii thus derived should be minimum energy features as well. To this purpose, a FORTRAN IV program, entitled EDEN, was written that, given the results of a GAUSSIAN single point calculation, calculates: 1) the total electron density within any plane specified by the user, 2) the minimum electron density along the vector between two bonded atoms, and, using this as the (3,-1) cp, 3) the bonded radii of all atoms in the molecule along all internuclear vectors. By Bader's (1971) definition, the bonded radius of an atom is the distance from the (3,-3) cp (the nuclear position) to the (3,-1) cp (the minimum along the bond path). In general, the (3,-1) cp is not constrained to lie on the internuclear vector. However, for simple molecules modelling single polyhedra, or several polyhedra linked at the corners, the assumption that the (3,-1) cp lies along the internuclear vector is probably a valid one.

Molecular Orbital Theory

For an electron with a spatial wave function $\psi_a(\mathbf{r})$, the electron density for that atom is simply the probability distribution function, $|\psi_a(\mathbf{r})|^2$. The total electron density, $\rho(\mathbf{r})$, for an N−electron system is found by summing the probability density functions over all N electrons. Since two electrons occupy each spatial wave state, this can be more easily written as

$$\rho(\mathbf{r}) = 2 \sum_a^{N/2} |\psi_a(\mathbf{r})|^2. \tag{1}$$

There are, however, no feasible numerical methods for calculating the molecular orbitals. Therefore, each spatial wave function is, in turn, written as a linear combination of a set of K known basis functions, called the basis set. This expansion is written as

$$\psi_i = \sum_{\mu=1}^{K} C_{\mu i} \phi_\mu \quad i = 1, 2, \cdots, K. \tag{2}$$

The coefficients, $C_{\mu i}$, are called the molecular orbital coefficients, and the ϕ_μ are the basis functions, or atomic orbitals. The problem of determining the Hartree-Fock molecular orbitals now becomes one of determining the molecular orbital coefficients. We can derive a computational form of the equation for $\rho(\mathbf{r})$ by inserting the molecular orbital expansion into equation (1),

$$
\begin{aligned}
\rho(\mathbf{r}) &= 2 \sum_a^{N/2} \psi_a^*(\mathbf{r}) \psi_a(\mathbf{r}) \\
&= 2 \sum_a^{N/2} \sum_\nu C_{\nu a}^* \phi_\nu^*(\mathbf{r}) \sum_\mu C_{\mu a} \phi_\mu(\mathbf{r}) \\
&= \sum_{\mu\nu} \left[2 \sum_a^{N/2} C_{\mu a} C_{\nu a}^* \right] \phi_\mu(\mathbf{r}) \phi_\nu^*(\mathbf{r}) \\
&= \sum_{\mu\nu} P_{\mu\nu} \phi_\mu(\mathbf{r}) \phi_\nu^*(\mathbf{r}).
\end{aligned}
\tag{3}
$$

The $P_{\mu\nu}$ are the elements of the *density matrix*, $\mathbf{P}$, and can be written in terms of the molecular orbital coefficients as follows,

29

$$P_{\mu\nu} = 2 \sum_{a}^{N/2} C_{\mu a} C_{\nu a}^* \tag{4}$$

In matrix form, $\mathbf{P}$ is written as $\mathbf{P} = \mathbf{CC}^*$. $\mathbf{C}$ is the matrix of molecular orbital coefficients and is expressed as follows

$$\mathbf{C} = \begin{pmatrix} C_{11} & C_{12} & \cdots & C_{1K} \\ C_{21} & C_{22} & \cdots & C_{2K} \\ \vdots & \vdots & & \vdots \\ C_{K1} & C_{K2} & \cdots & C_{KK} \end{pmatrix} \tag{5}$$

The columns of $\mathbf{C}$ are the molecular orbital coefficients of the molecular orbitals (i.e. $\psi_1 = C_{11}\phi_1 1 + C_{21}\phi_2 + \cdots + C_{K1}\phi_K$). Since the $C_{\mu\nu}$ are real valued when gaussian basis functions are used, the density matrix is written as

$$\mathbf{P} = \mathbf{CC}^t \tag{6}$$

Using equation (6), the expression for $\rho(\mathbf{r})$ can be written as

$$\rho(\mathbf{r}) = \Phi^t \mathbf{P} \Phi$$
$$= \Phi^t (\mathbf{CC}^t) \Phi \tag{7}$$

where Φ is the vector of the K atomic orbital basis functions. This form of the equation is convenient as it can be easily programmed. Furthermore, the molecular orbital coefficients and the density matrix are provided by GAUSSIAN output and since the basis set is known prior to any molecular orbital coefficients, Φ can be easily constructed.

Appendix B

CALCULATED AND PROMOLECULE ELECTRON DENSITY MAPS
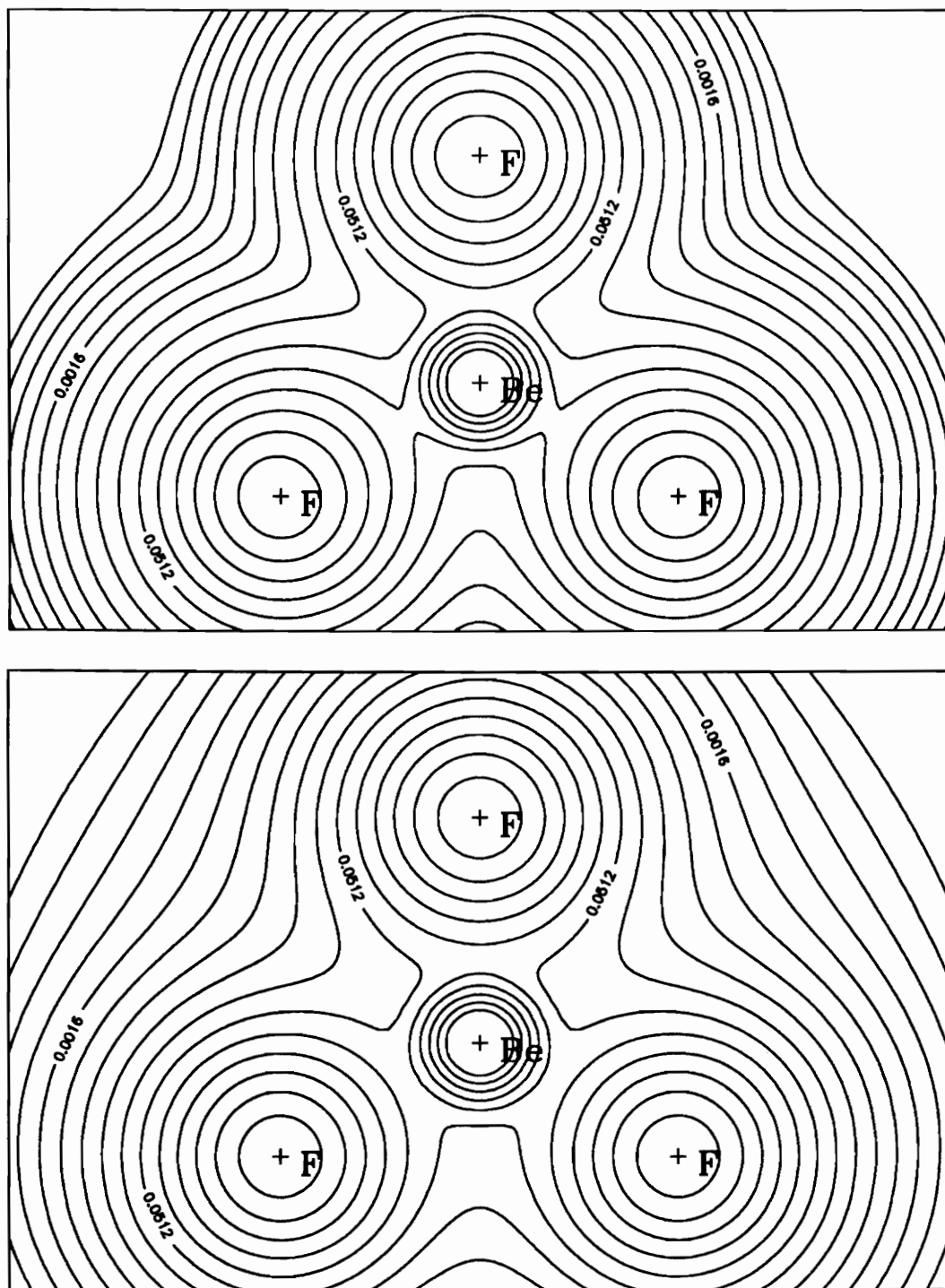
Figure B1. (a) Total electron density map for HBeF$_3$ and (b) promolecule electron density map for BeF$_3$. The contour interval is 0.0001, 0.0002, 0.0004, ...,e/b^3. The maps are 6.0 X 4.0Å.
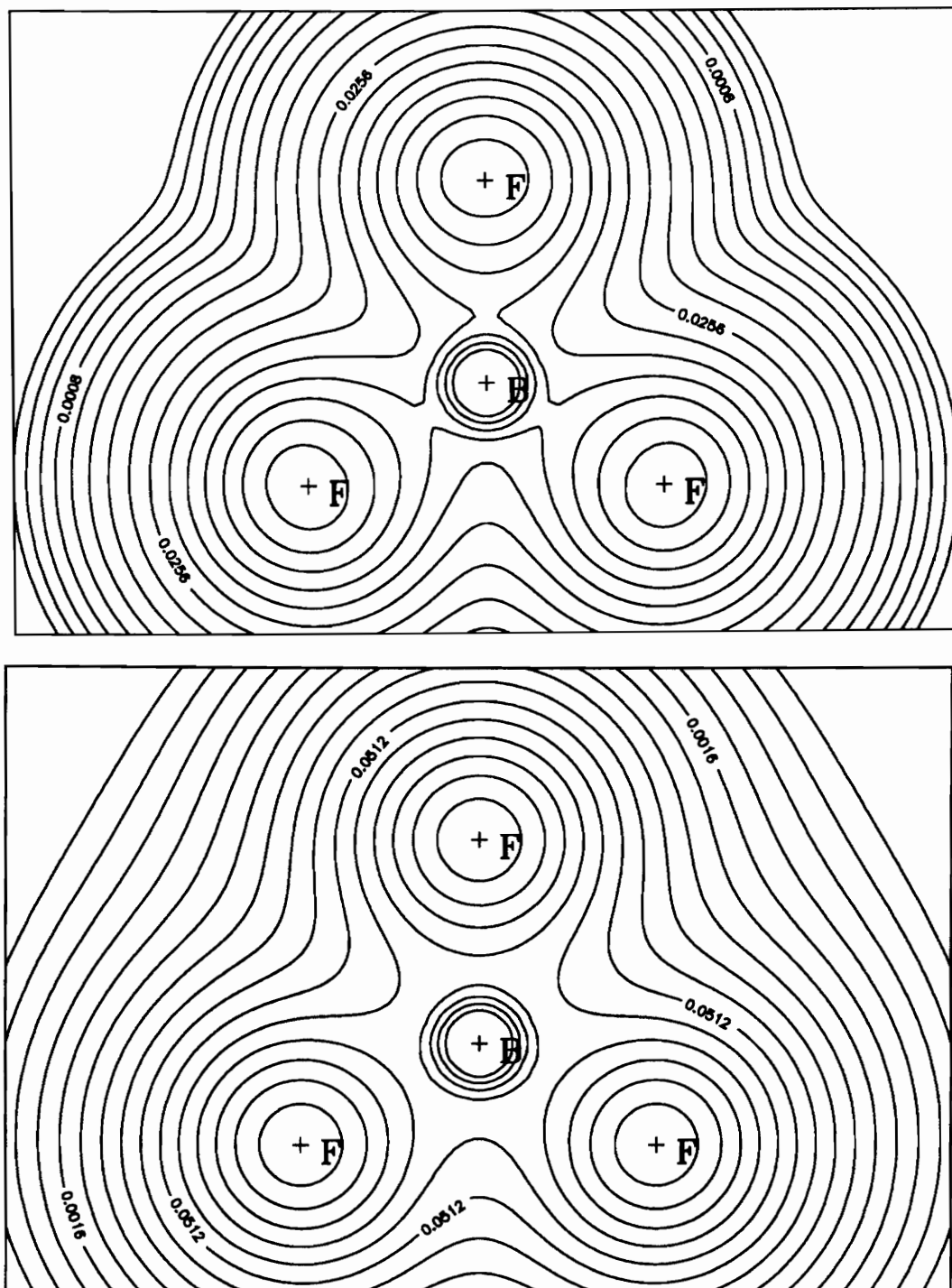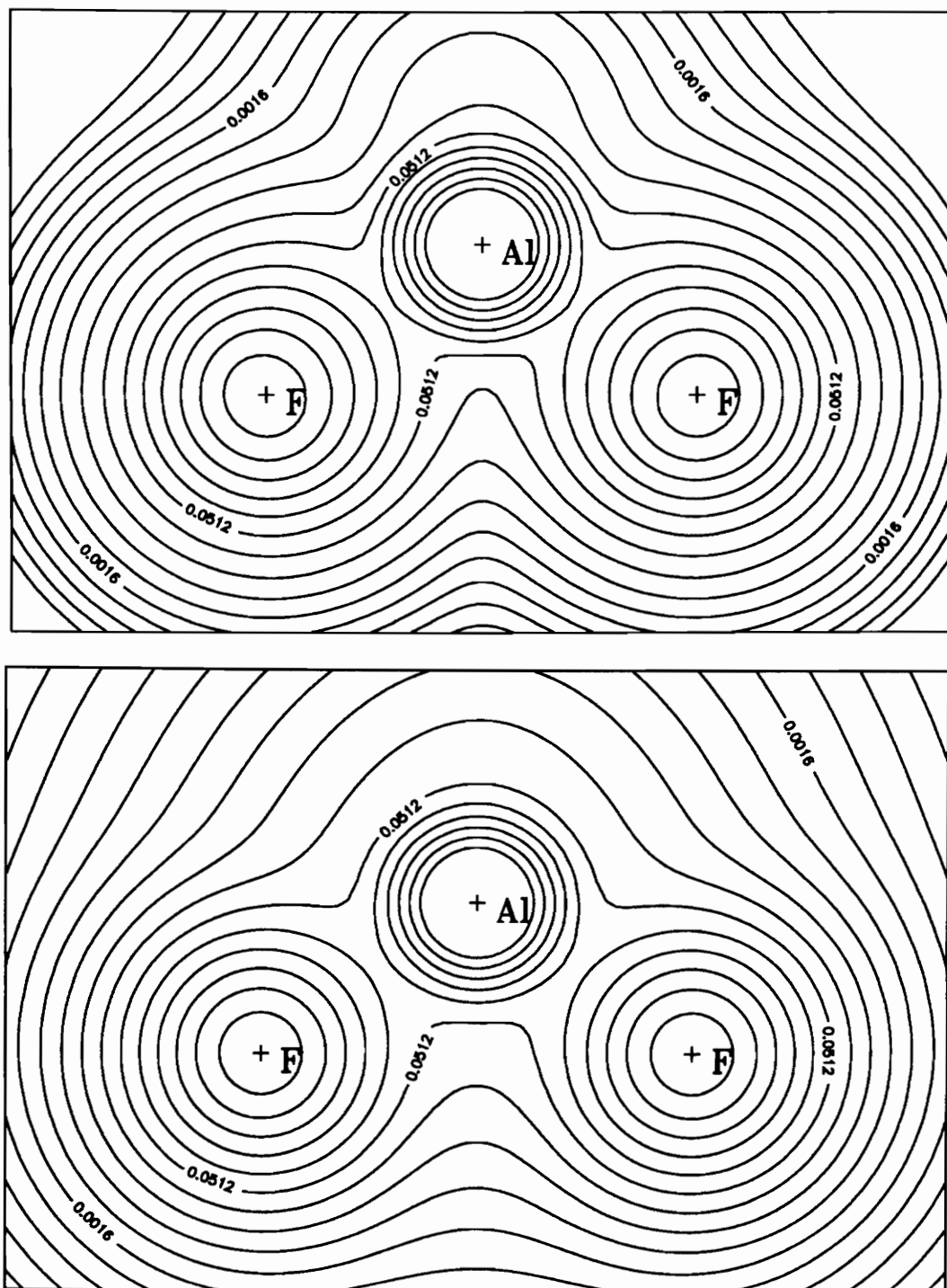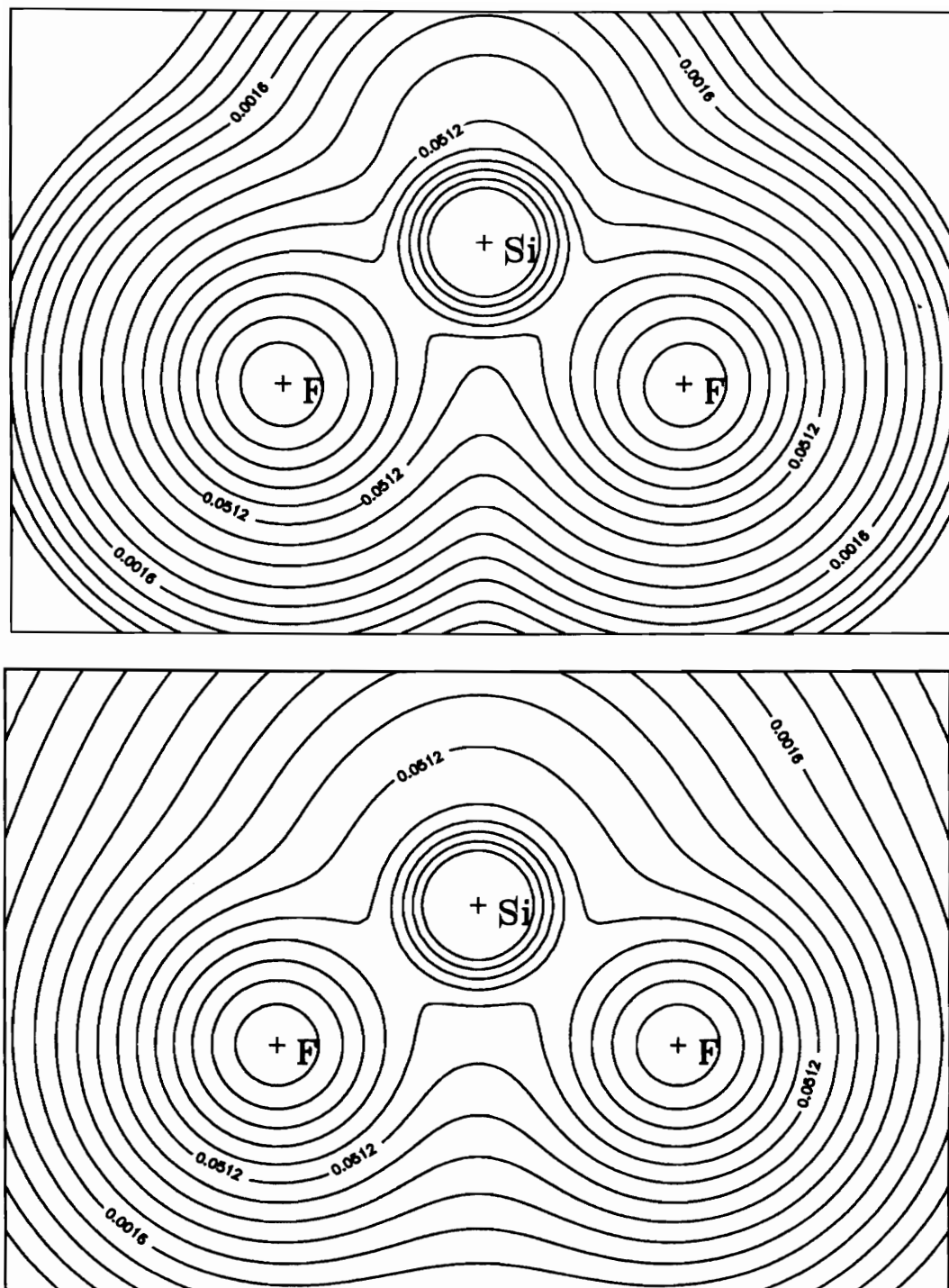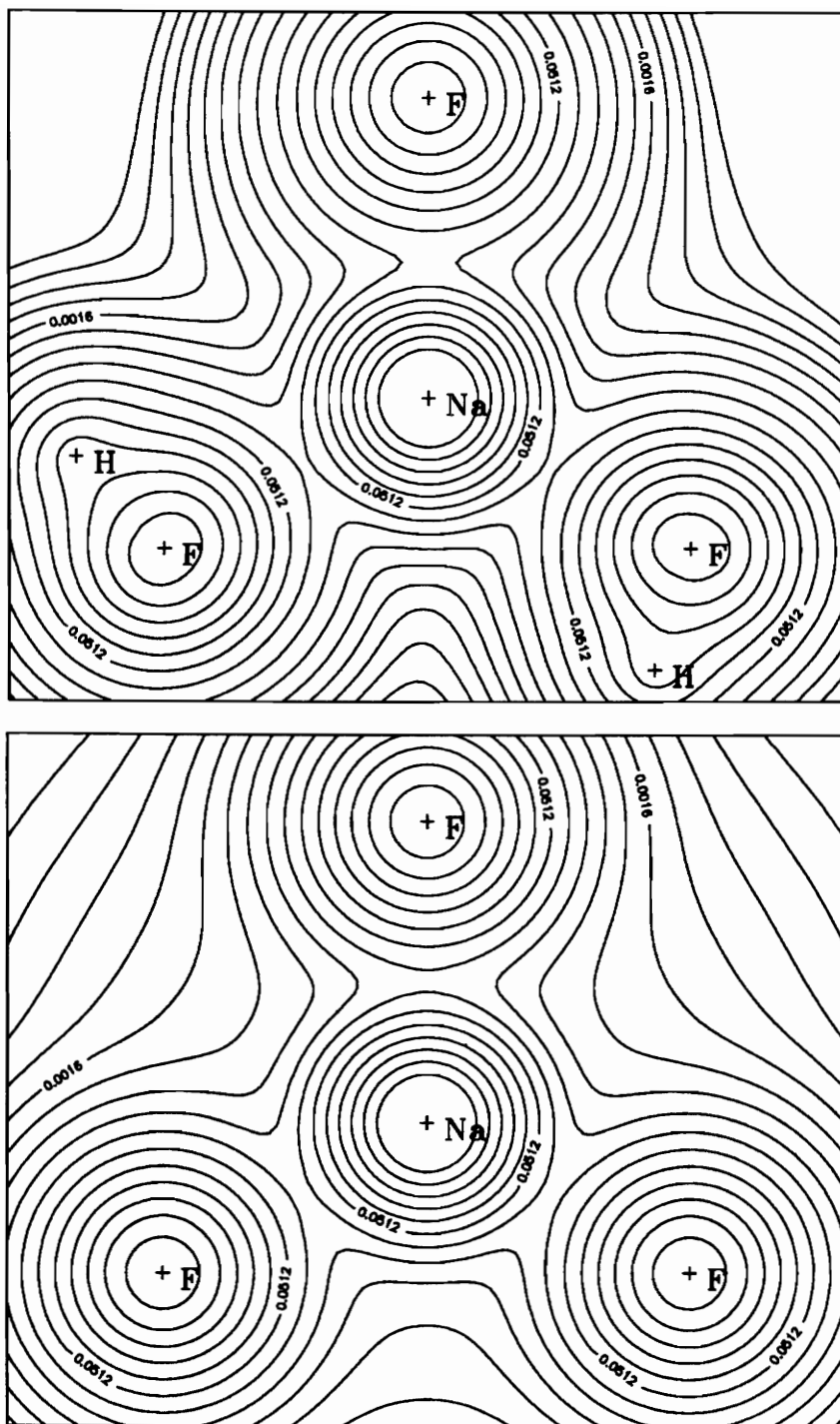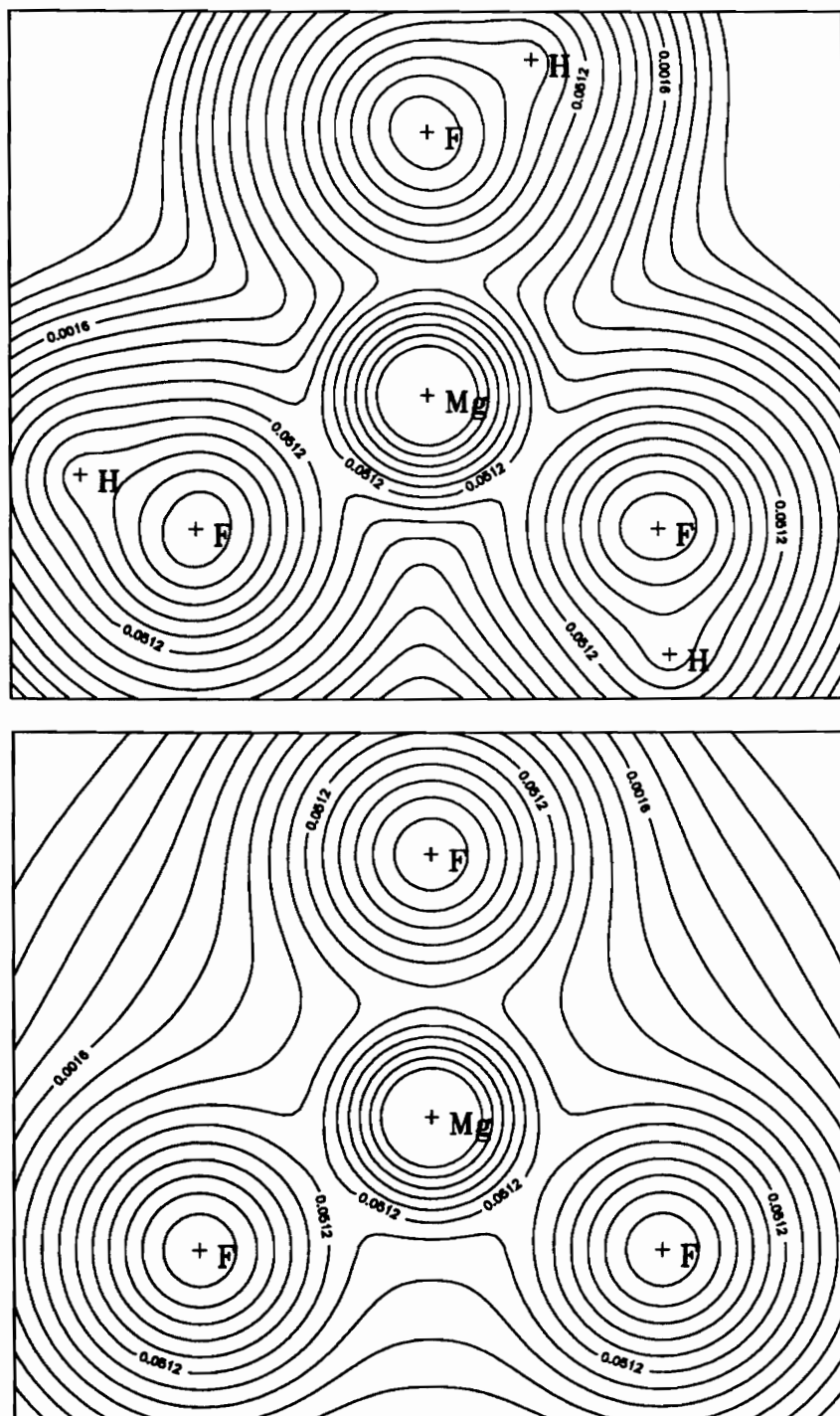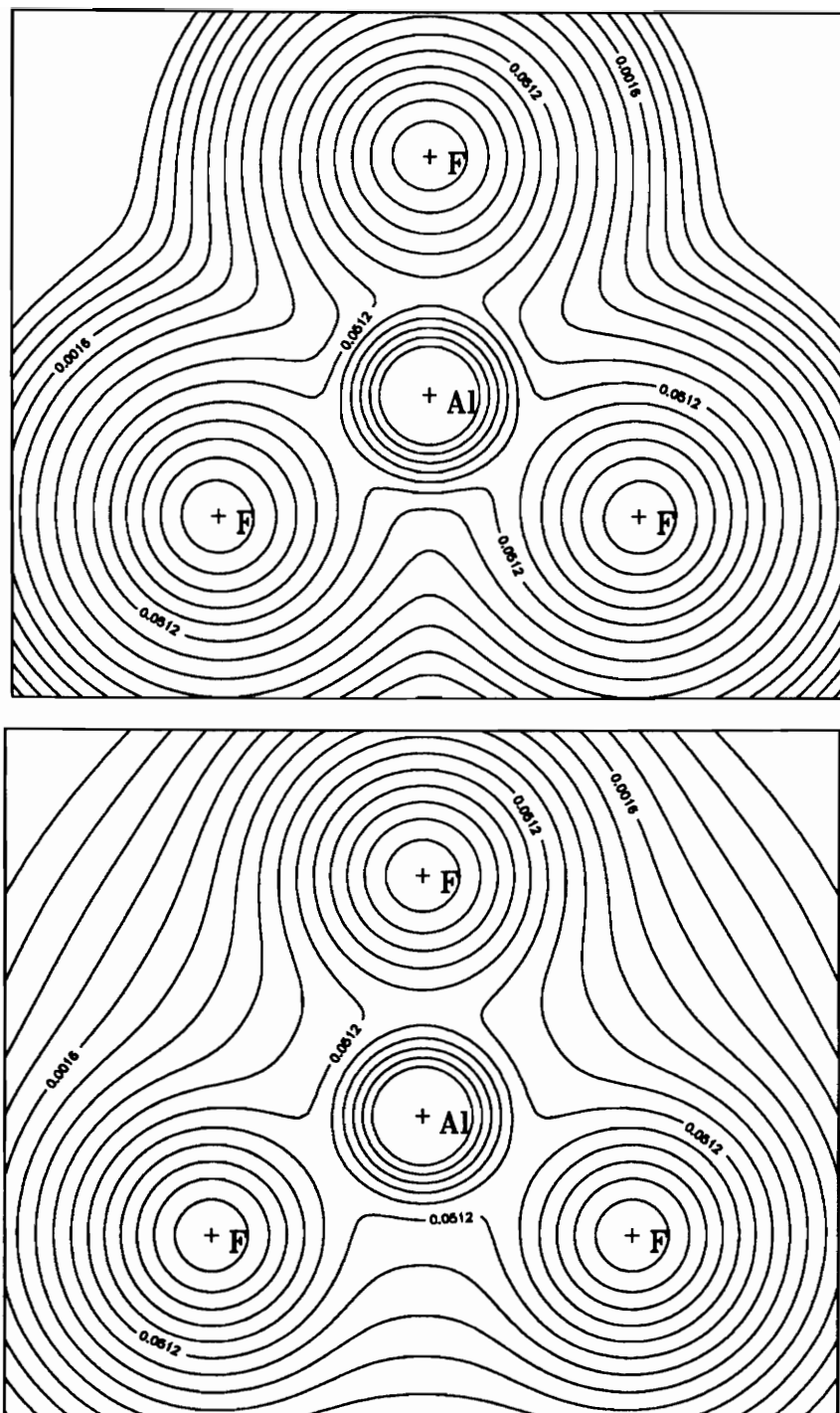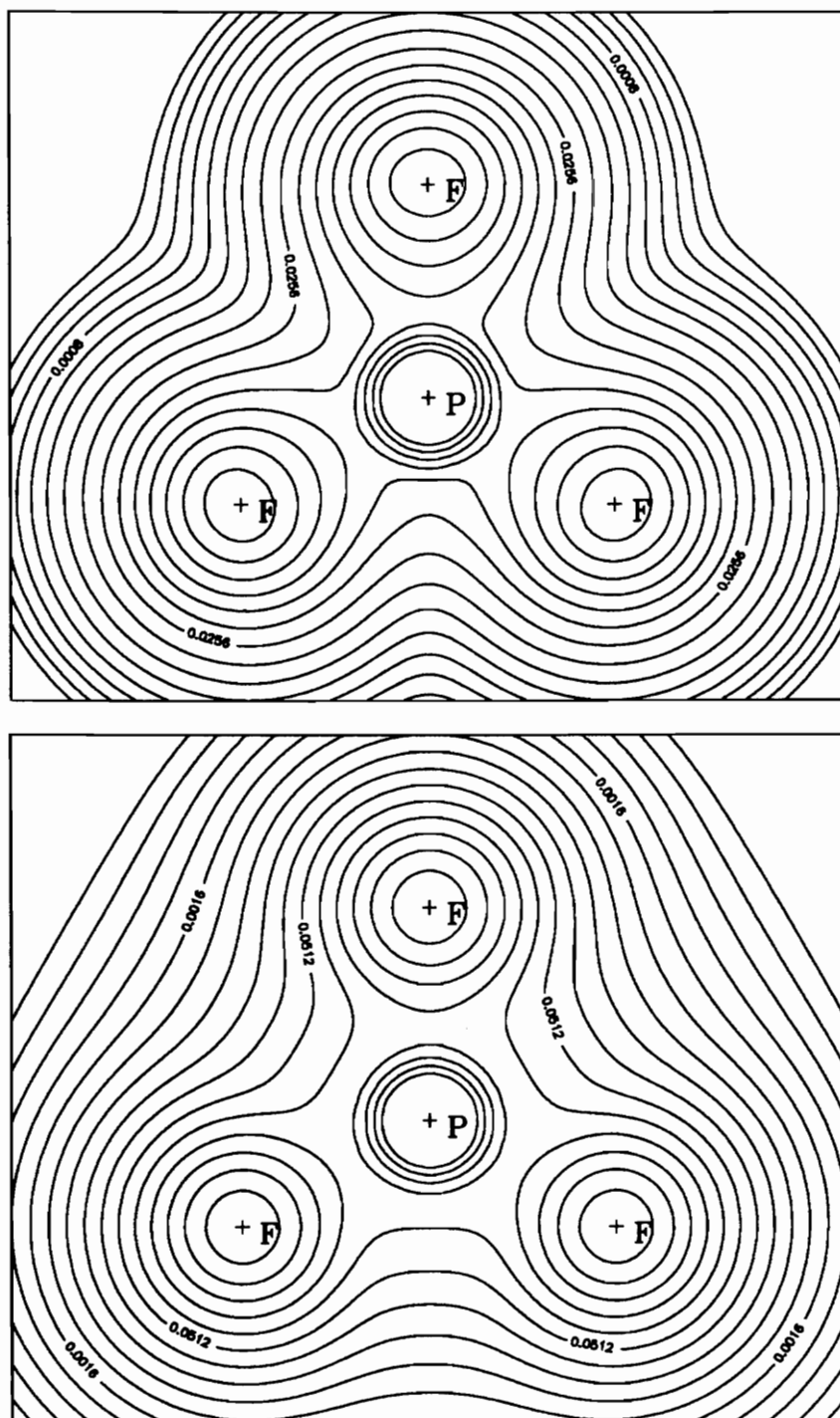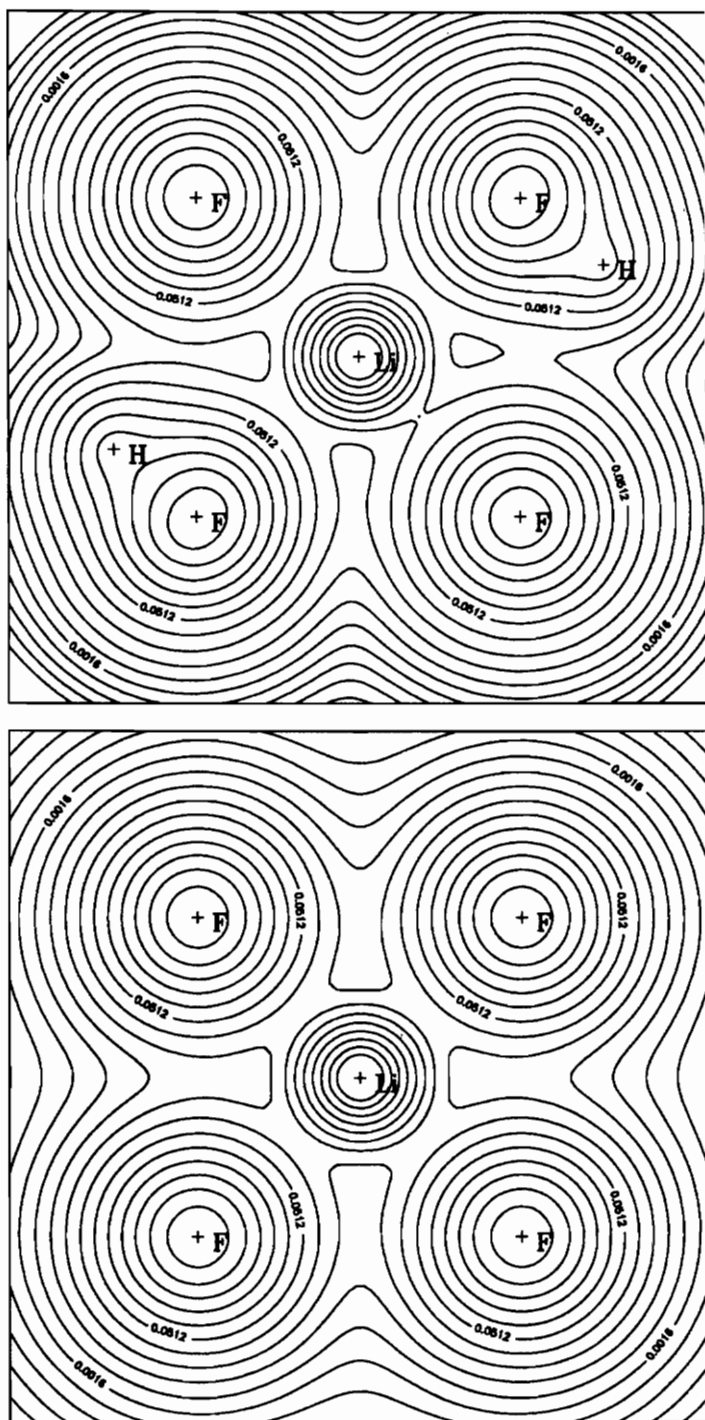
Figure B2. (a) Total electron density map and (b) promolecule electron density map for BF_3. The contour interval is 0.0001, 0.0002, 0.0004, ...,e/b^3. The maps are 6.0 X 4.0Å.
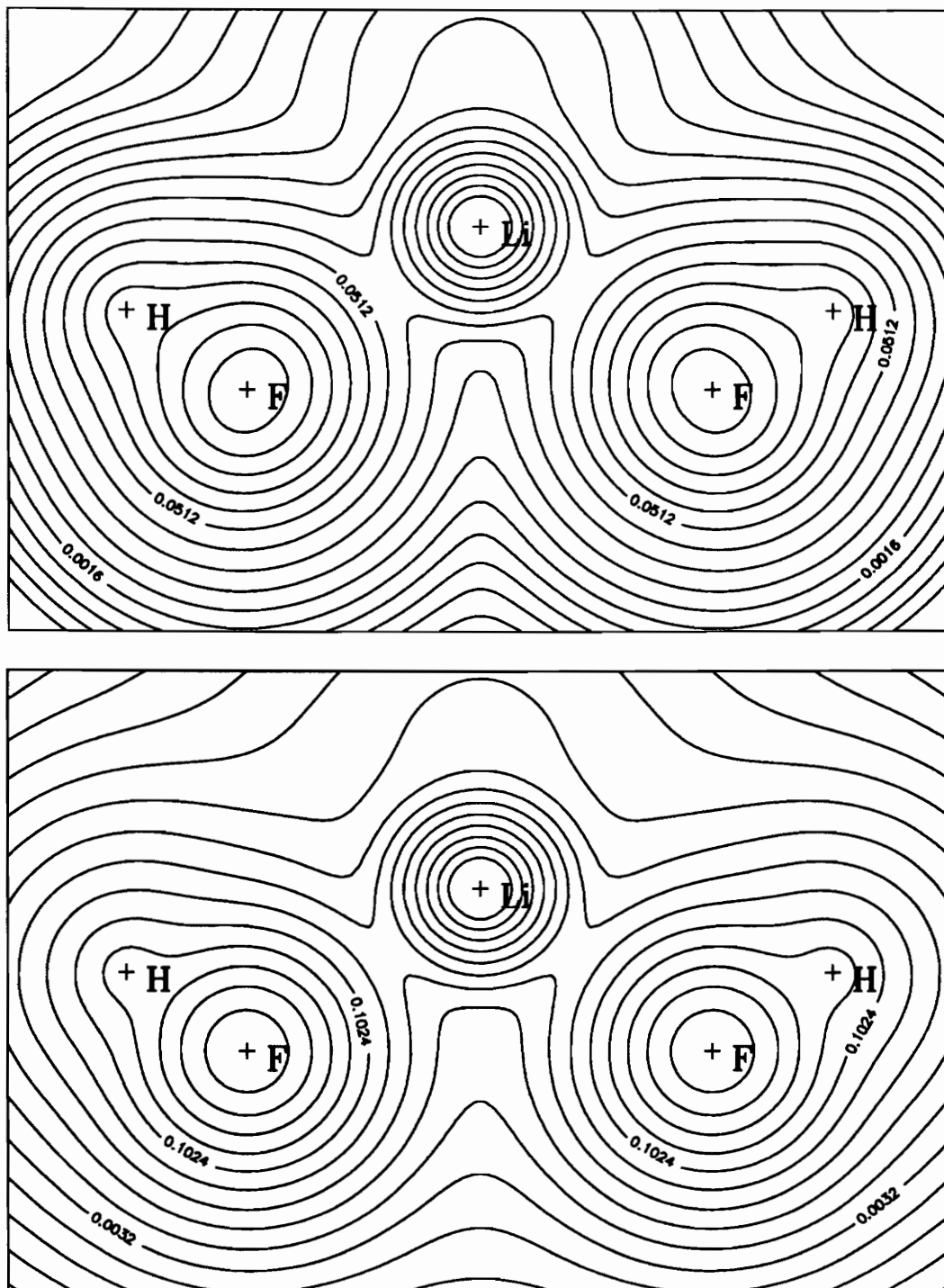
Figure B3. (a) Total electron density map and (b) promolecule electron density map for H_3LiF_4. The contour interval is 0.0001, 0.0002, 0.0004, ...,e/b^3. The maps are 6.0 X 4.0Å.
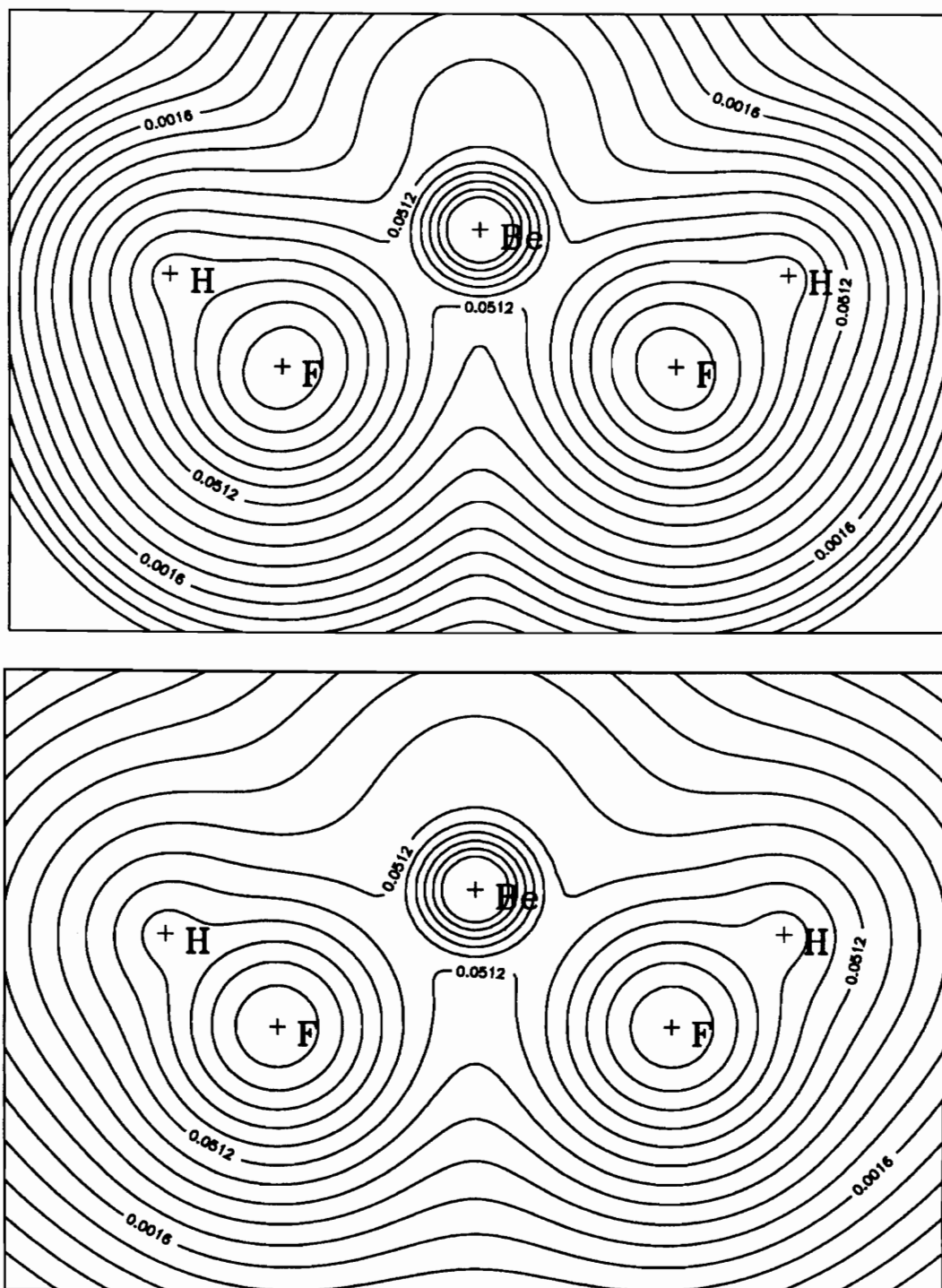
Figure B4. (a) Total electron density map and (b) promolecule electron density map for H_2BeF_4. The contour interval is 0.0001, 0.0002, 0.0004, ...,e/b^3. The maps are 6.0 X 4.0Å.
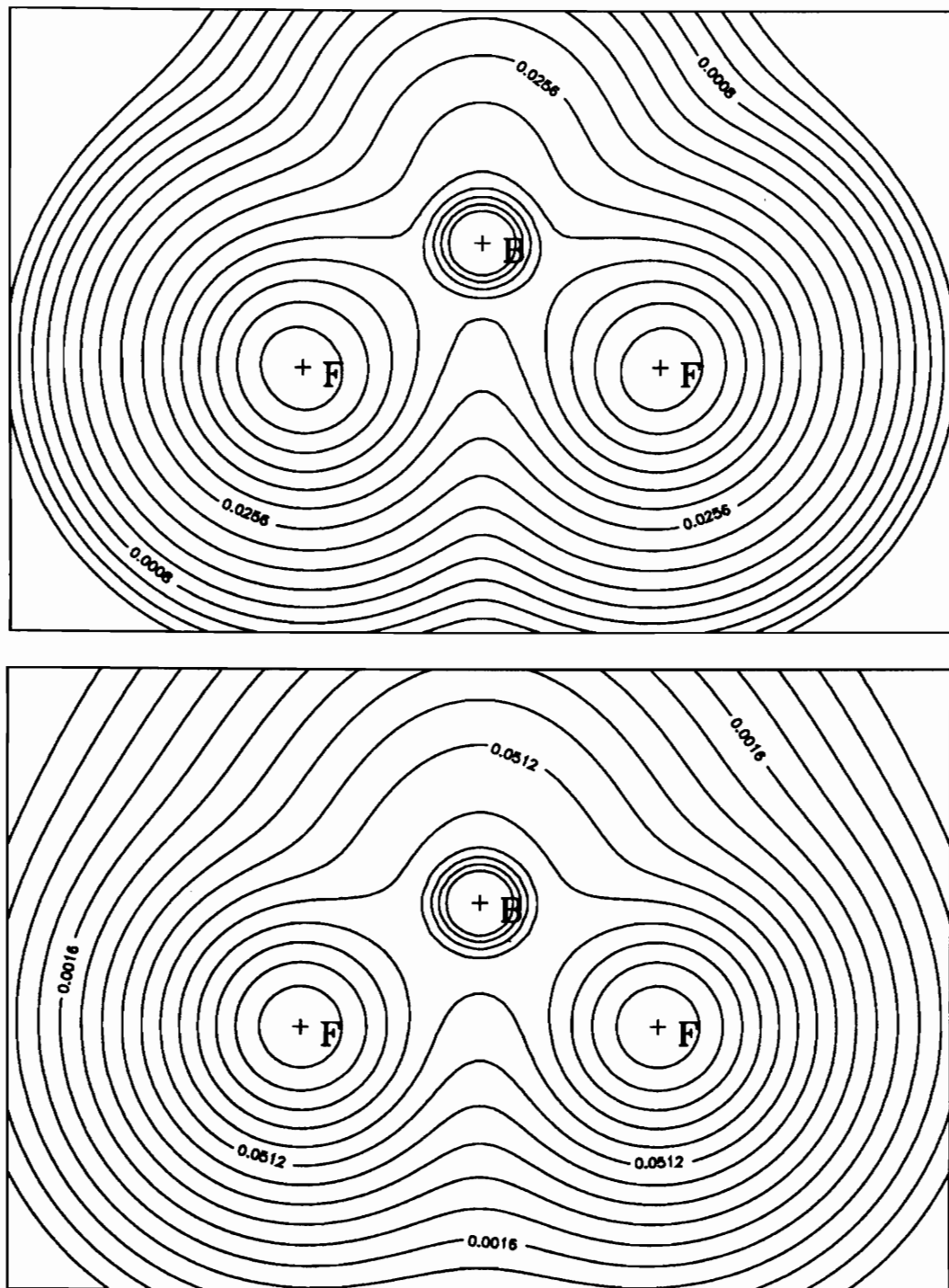
Figure B5. (a) Total electron density map and (b) promolecule electron density map for HBF_4. The contour interval is $0.0001, 0.0002, 0.0004, \ldots, e/b^3$. The maps are $6.0 \times 4.0 \text{Å}$.
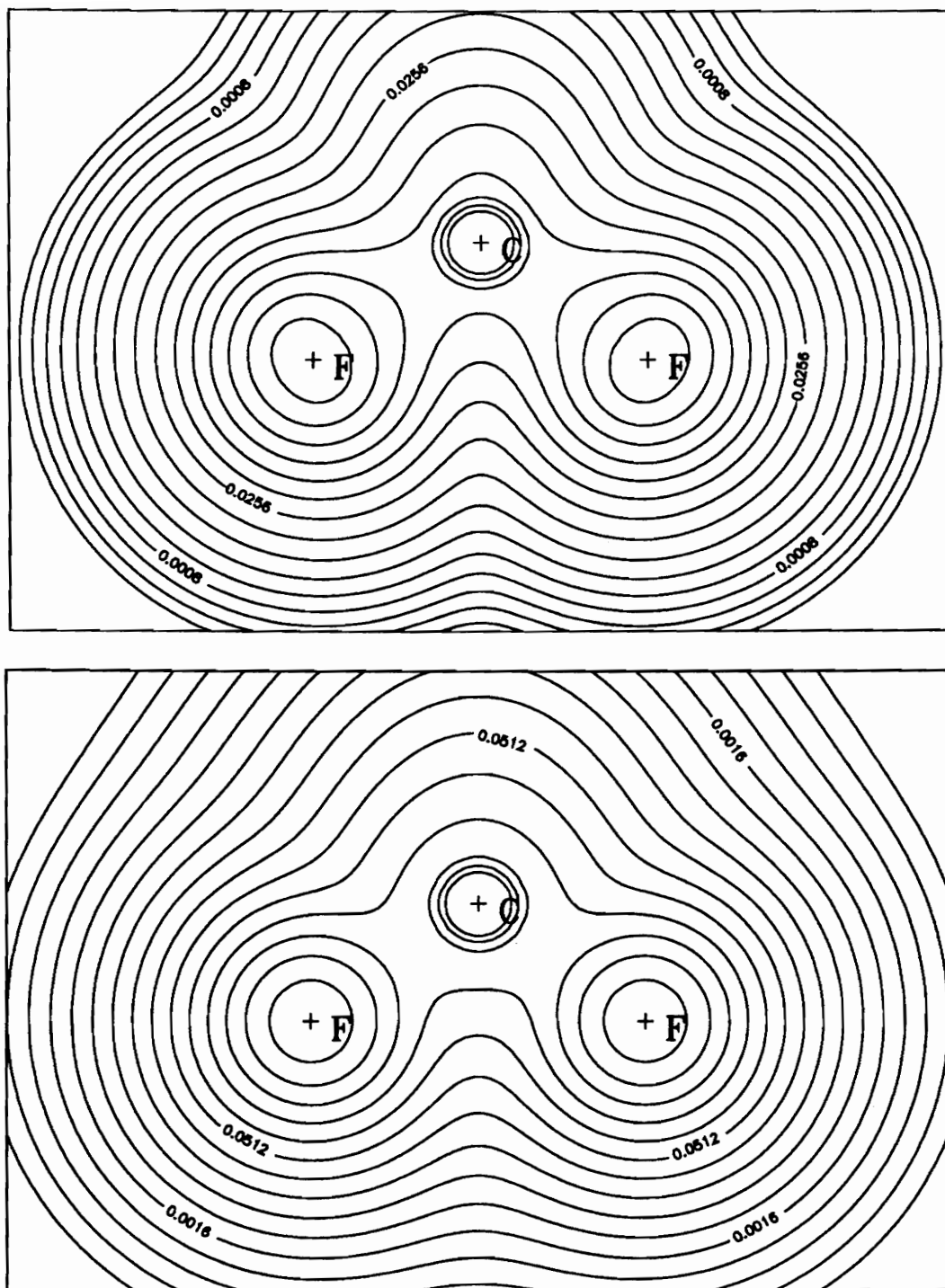
Figure B6. (a) Total electron density map and (b) promolecule electron density map for CF_4. The contour interval is 0.0001, 0.0002, 0.0004, ...,e/b^3. The maps are 6.0 X 4.0Å.
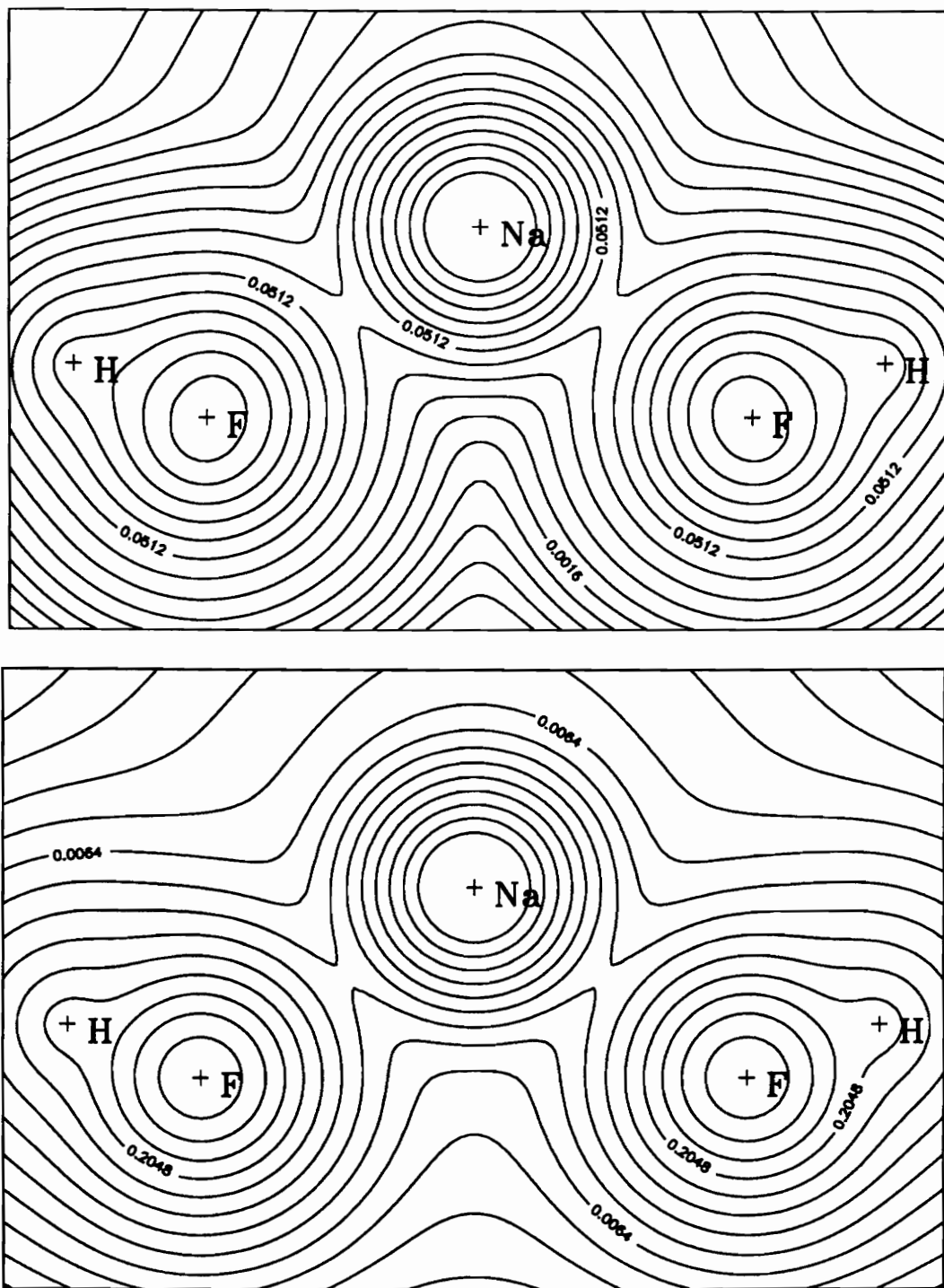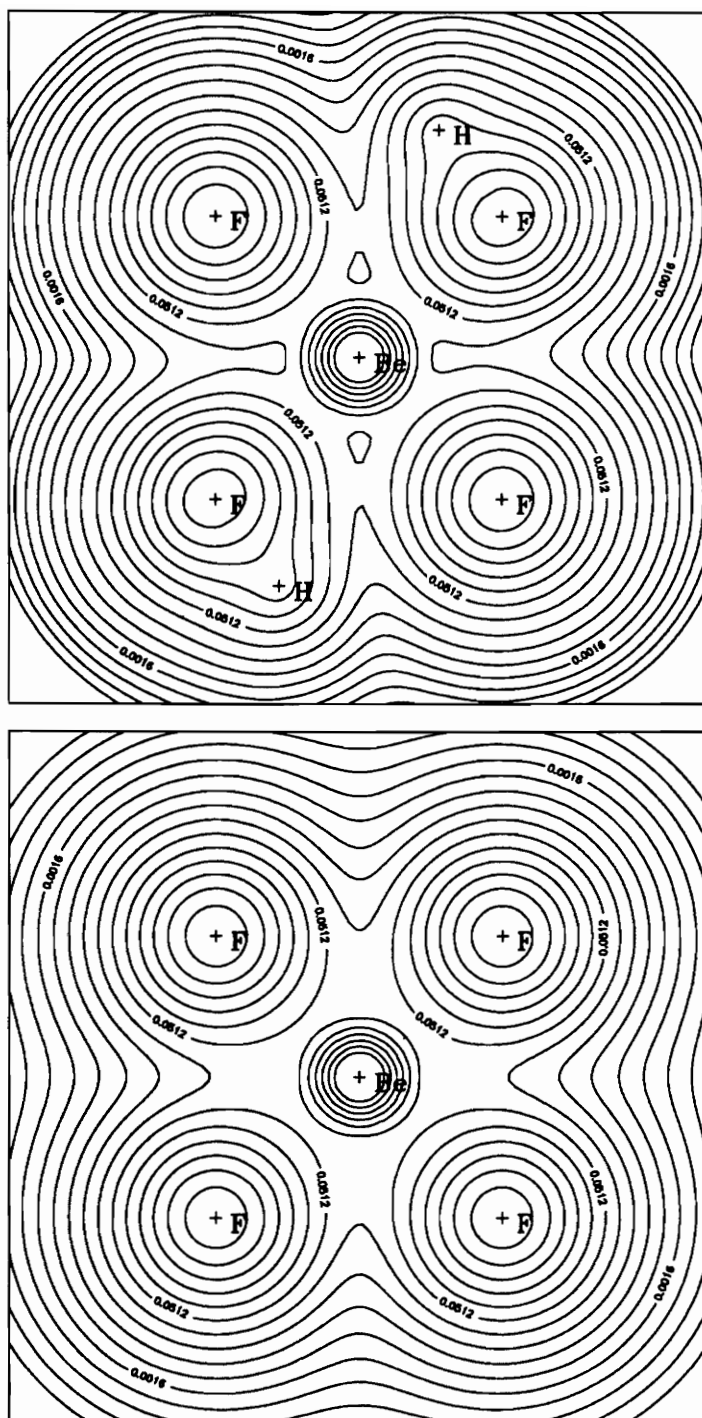
Figure B7. (a) Total electron density map and (b) promolecule electron density map for H_3NaF_4. The contour interval is 0.0001, 0.0002, 0.0004, ...,e/b^3. The maps are 6.0 X 4.0Å.
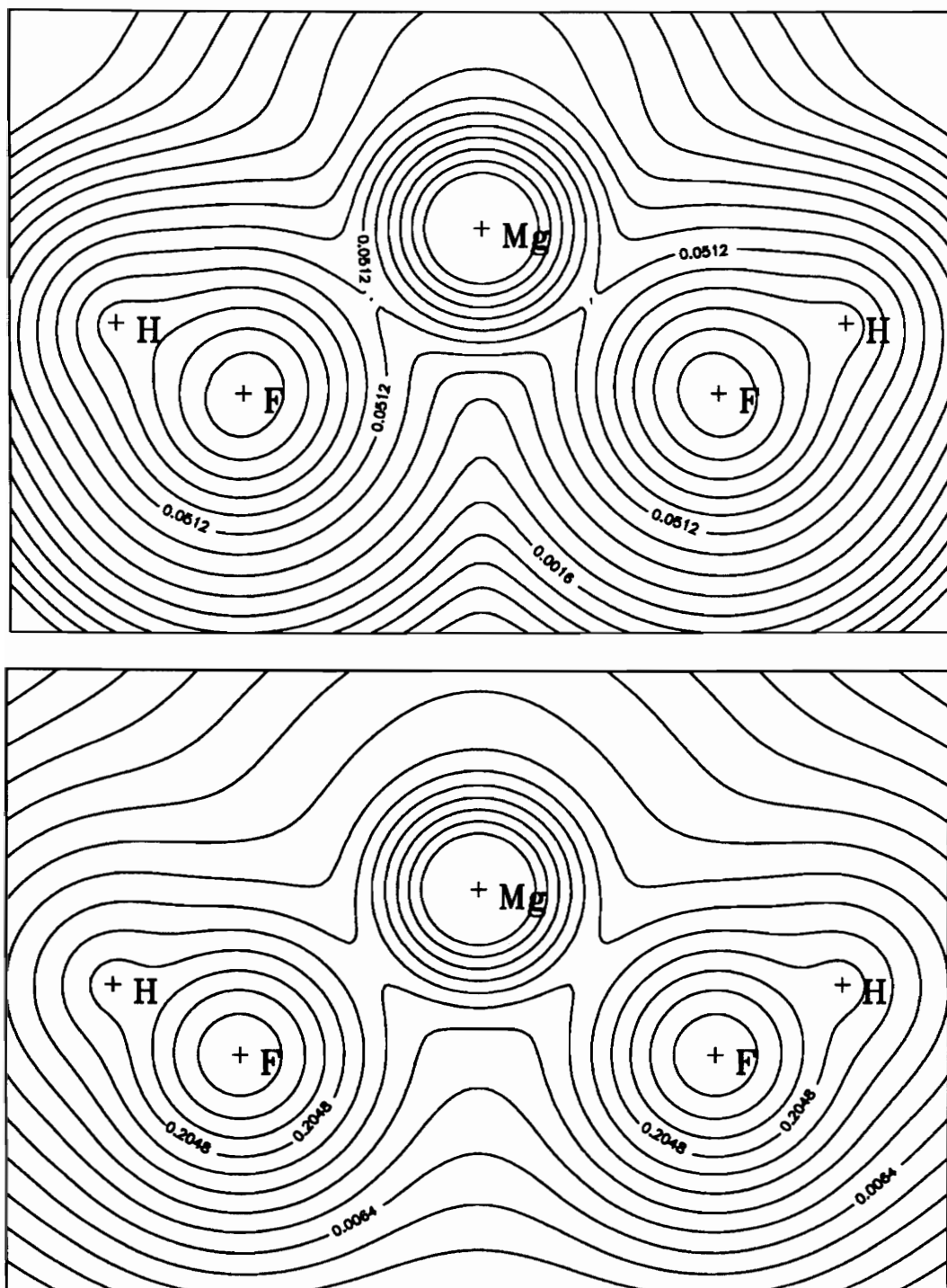
Figure B8. (a) Total electron density map and (b) promolecule electron density map for H_2MgF_4. The contour interval is 0.0001, 0.0002, 0.0004, ...,e/b^3. The maps are 6.0 X 4.0Å.
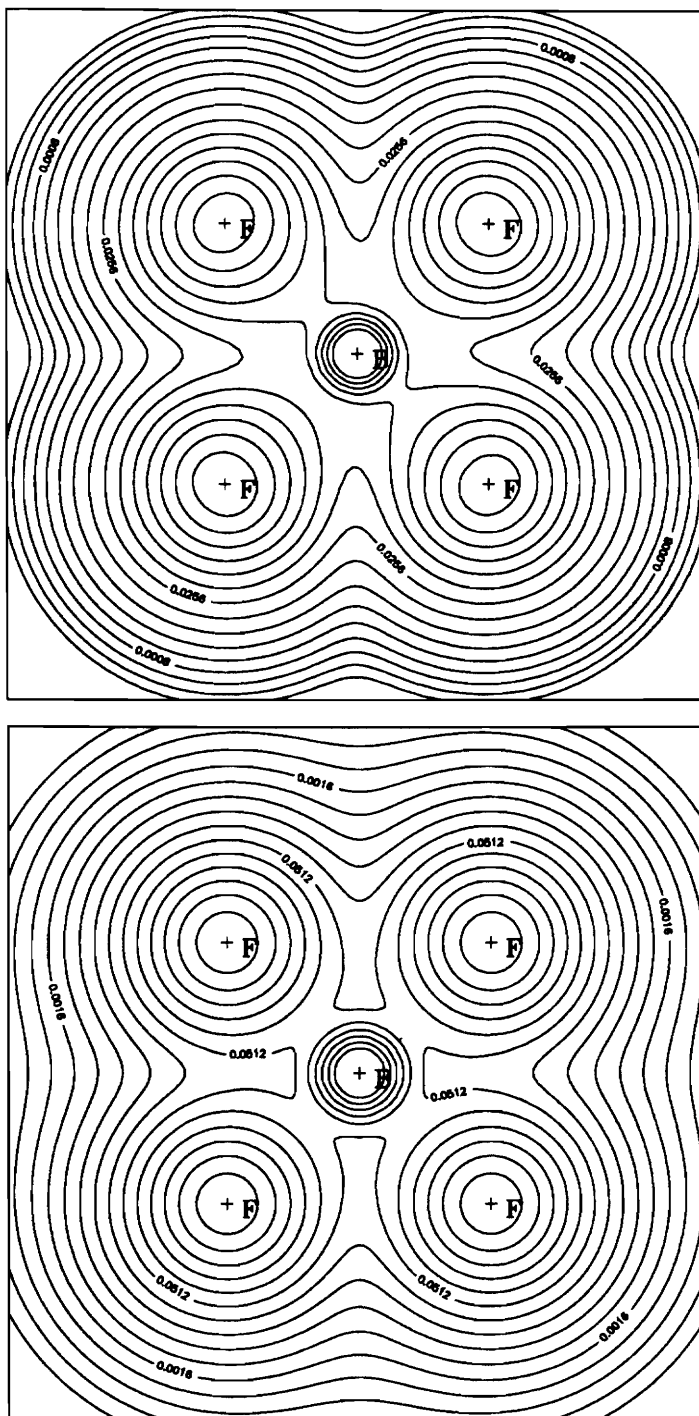
Figure B9. (a) Total electron density map and (b) promolecule electron density map for HAlF$_4$. The contour interval is 0.0001, 0.0002, 0.0004, ...,e/b^3. The maps are 6.0 X 4.0Å.

Figure B10. (a) Total electron density map and (b) promolecule electron density map for SiF$_4$. The contour interval is 0.0001, 0.0002, 0.0004, ... ,e/b^3. The maps are 6.0 X 4.0Å.
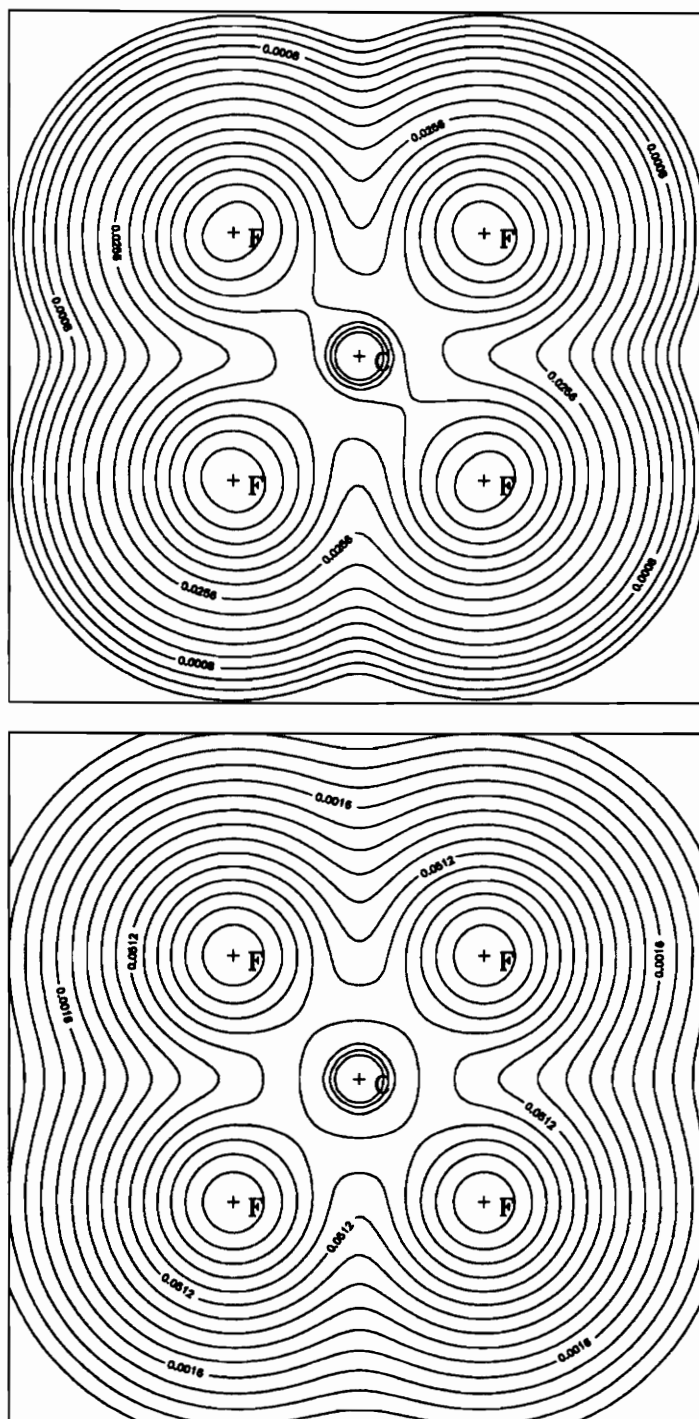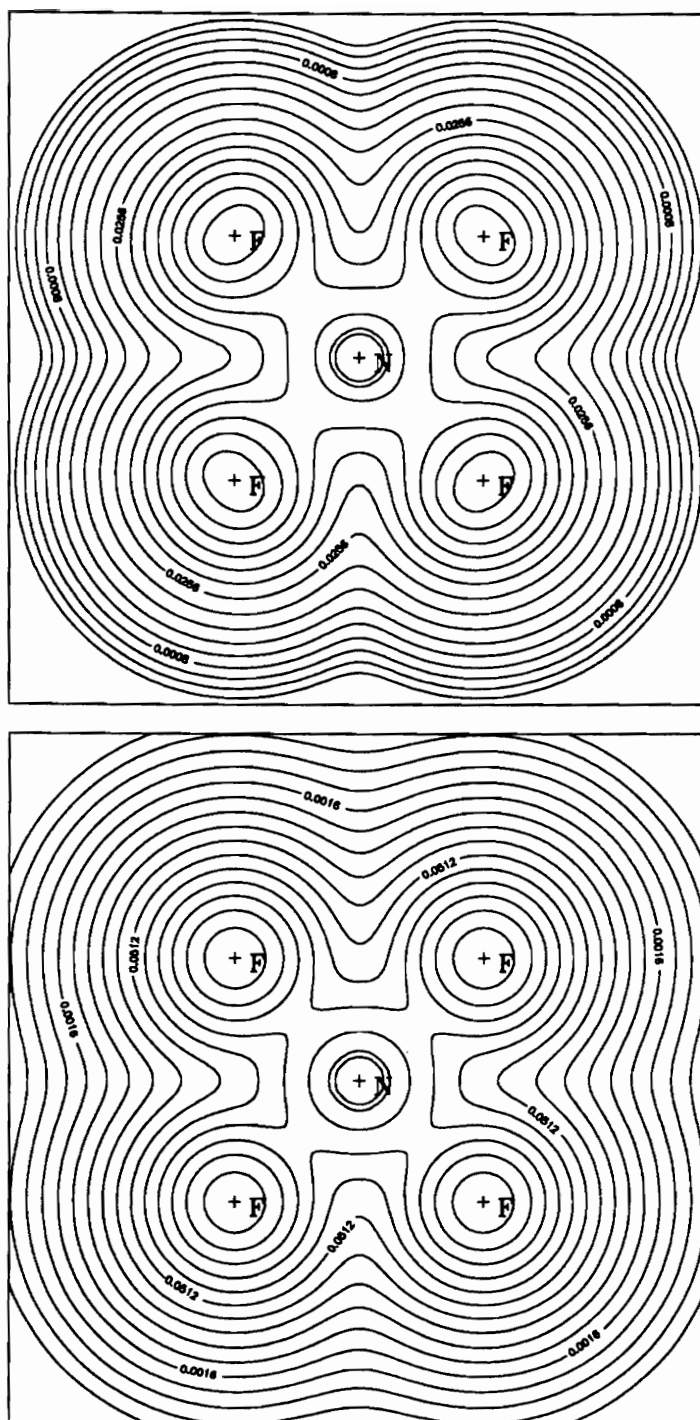
Figure B11. (a) Total electron density map for H_4NaF_5 and (b) promolecule electron density map for NaF_5. The contour interval is 0.0001, 0.0002, 0.0004, ...,e/b^3. The maps are 6.0 X 5.0Å.
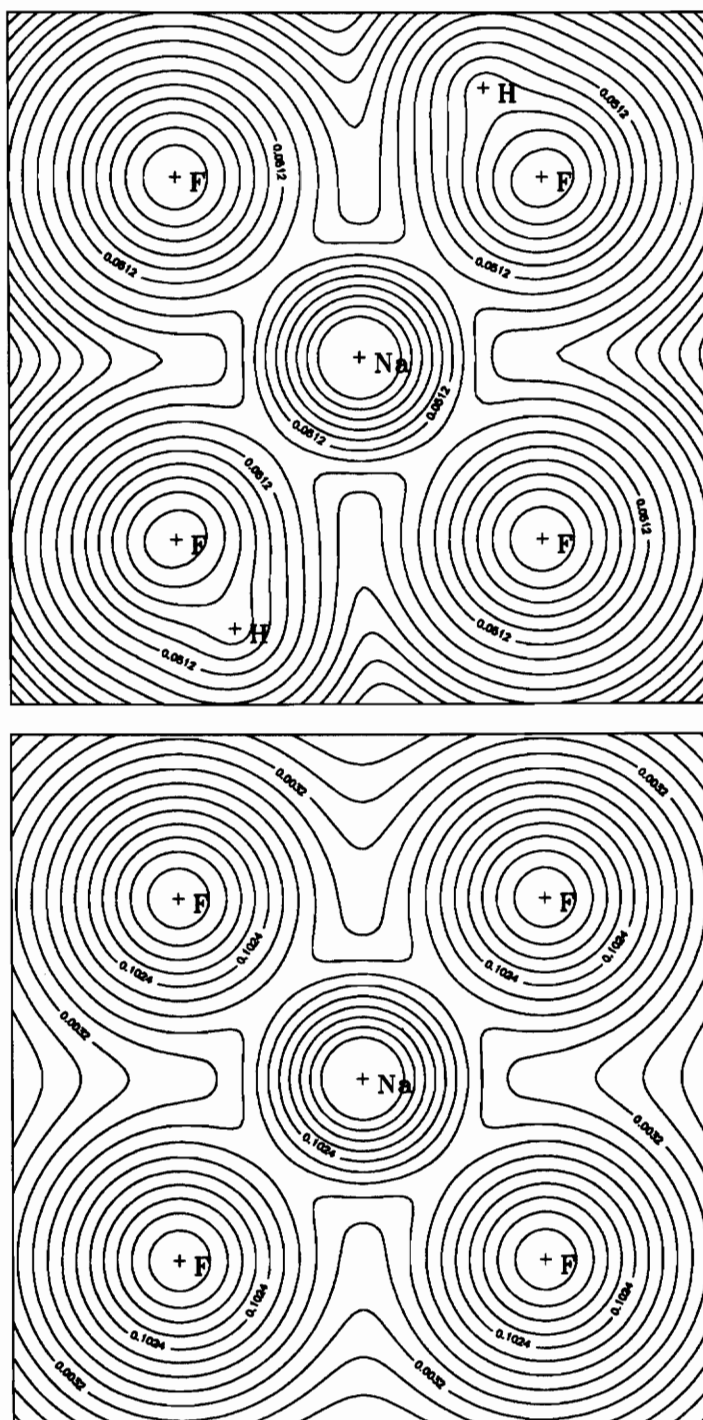
Figure B12. (a) Total electron density map for H_3MgF_5 and (b) promolecule electron density map for MgF_5. The contour interval is 0.0001, 0.0002, 0.0004, . . . ,e/b^3. The maps are 6.0 X 5.0Å.

43

Figure B13. (a) Total electron density map for H_2AlF_5 and (b) promolecule electron density map for AlF_5. The contour interval is 0.0001, 0.0002, 0.0004, ...,e/b^3. The maps are 6.0 X 5.0Å.
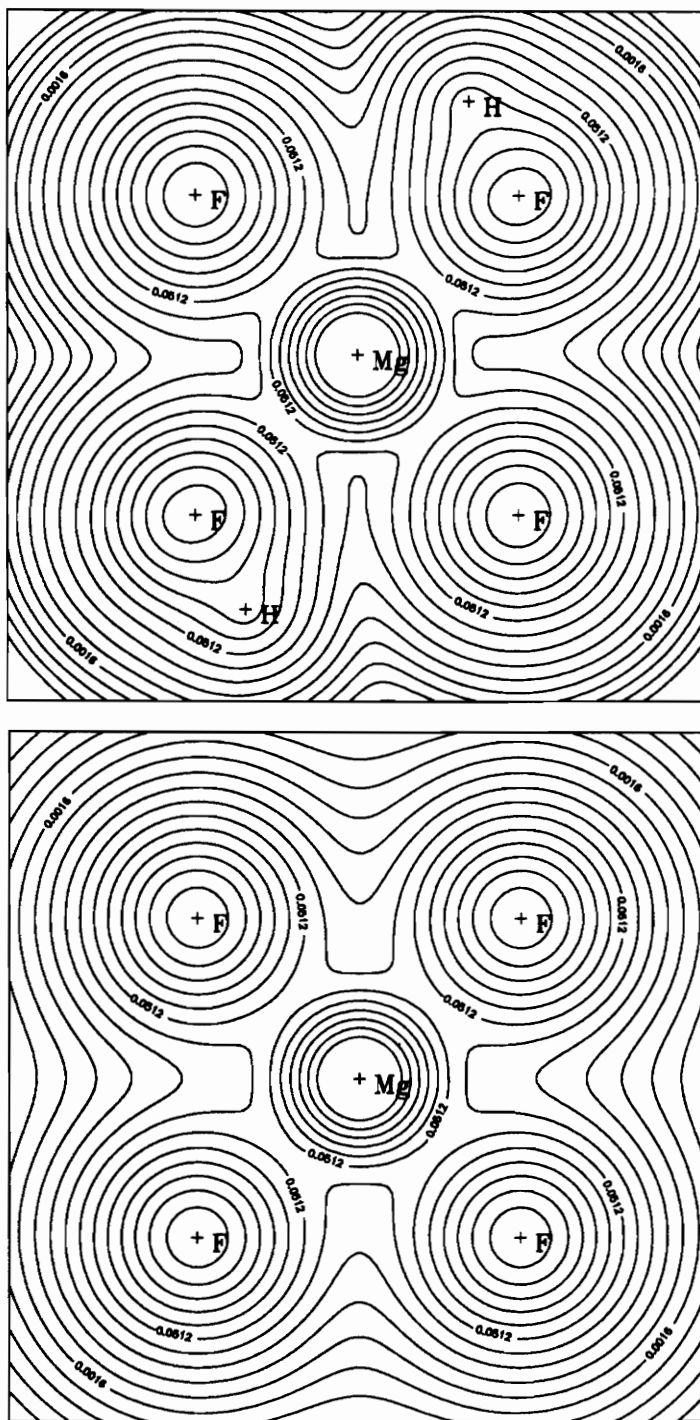
Figure B14. (a) Total electron density map and (b) promolecule electron density map for PF_5. The contour interval is 0.0001, 0.0002, 0.0004, ...,e/b^3. The maps are 6.0 X 5.0Å.

Figure B15. (a) Total electron density map for H_5LiF_6 and (b) promolecule electron density map for LiF_6. The contour interval is 0.0001, 0.0002, 0.0004, ...,e/b^3. The maps are 6.0 X 6.0Å.
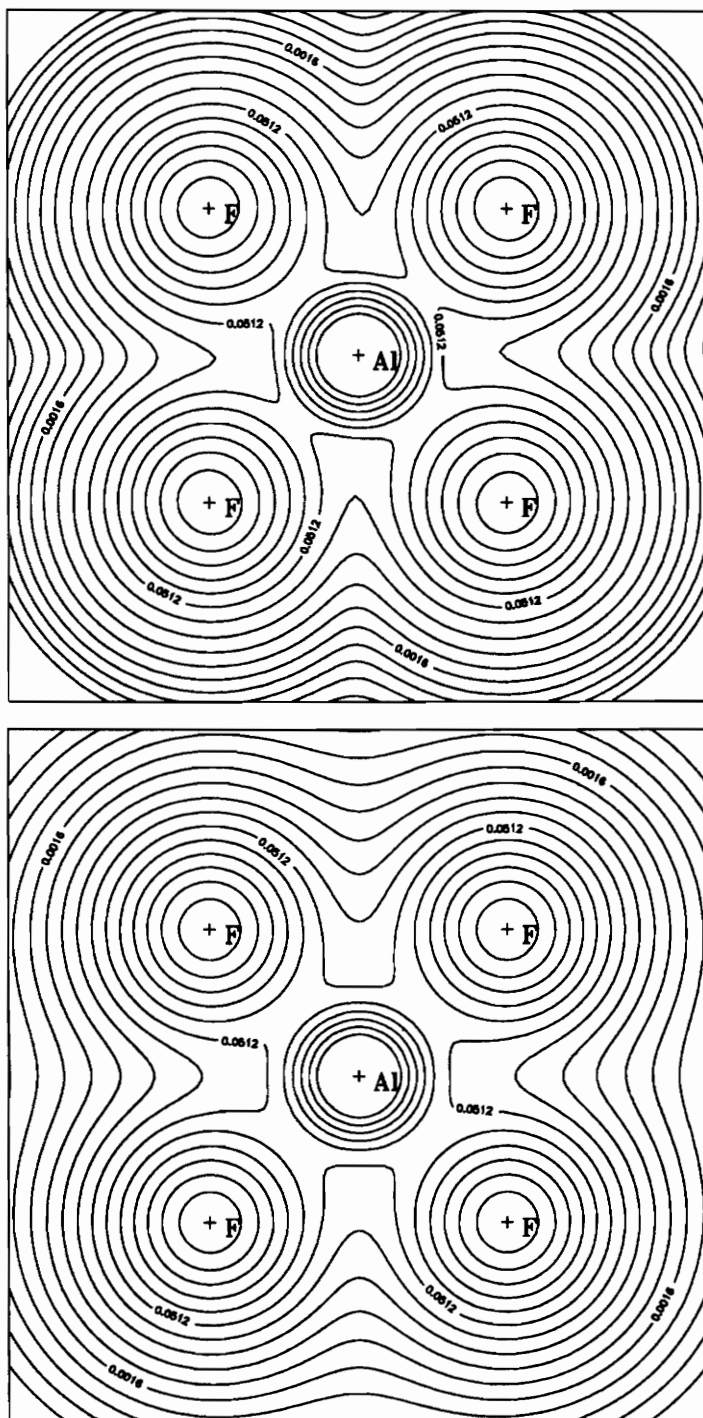
Figure B16. (a) Total electron density map for H_4BeF_6 and (b) promolecule electron density map for BeF_6. The contour interval is 0.0001, 0.0002, 0.0004, ...,e/b^3. The maps are 6.0 X 6.0Å.

Figure B17. (a) Total electron density map for H_3BF_6 and (b) promolecule electron density map for BF_6. The contour interval is 0.0001, 0.0002, 0.0004, ...,e/b^3. The maps are 6.0 X 6.0Å.
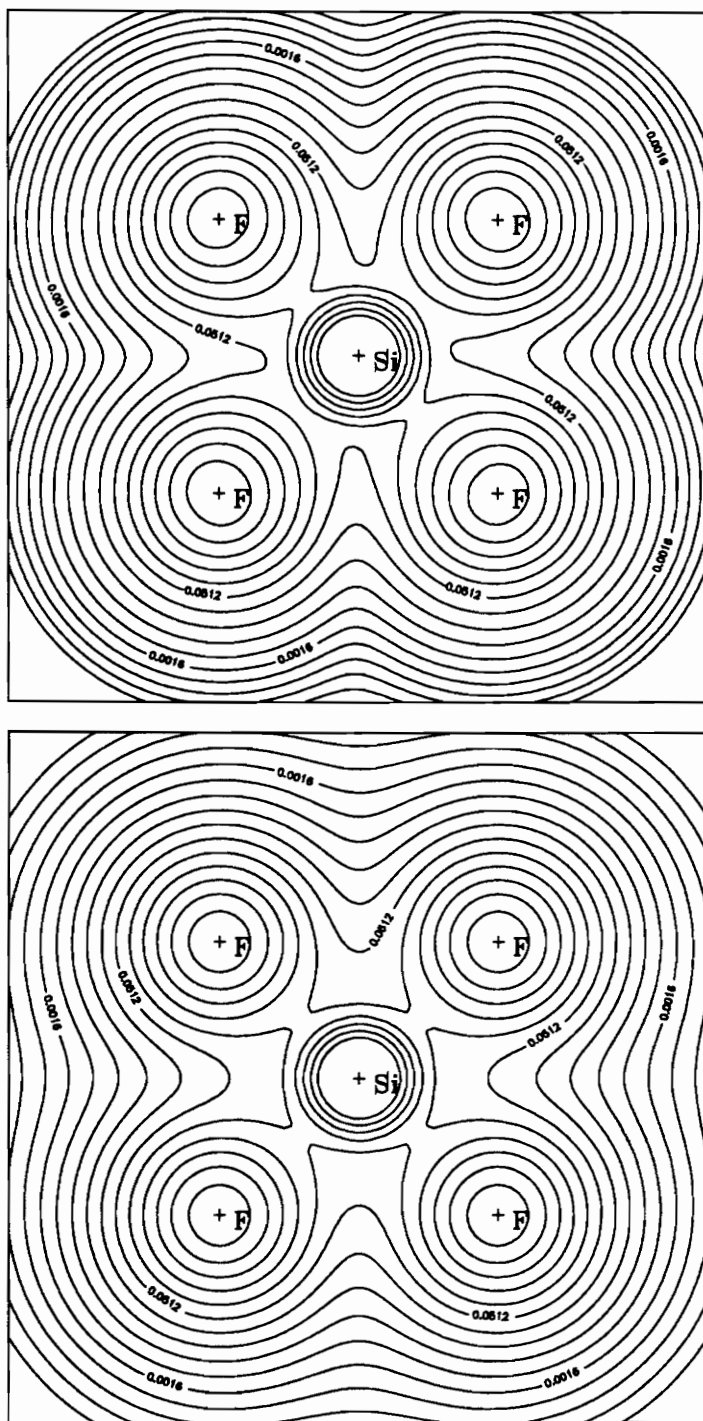
Figure B18. (a) Total electron density map for H_2CF_6 and (b) promolecule electron density map for CF_6. The contour interval is 0.0001, 0.0002, 0.0004, ... ,e/b^3. The maps are 6.0 X 6.0Å.

Figure B19. (a) Total electron density map for HNF_6 and (b) promolecule electron density map for NF_6. The contour interval is 0.0001, 0.0002, 0.0004, ...,e/b^3. The maps are 6.0 X 6.0Å.
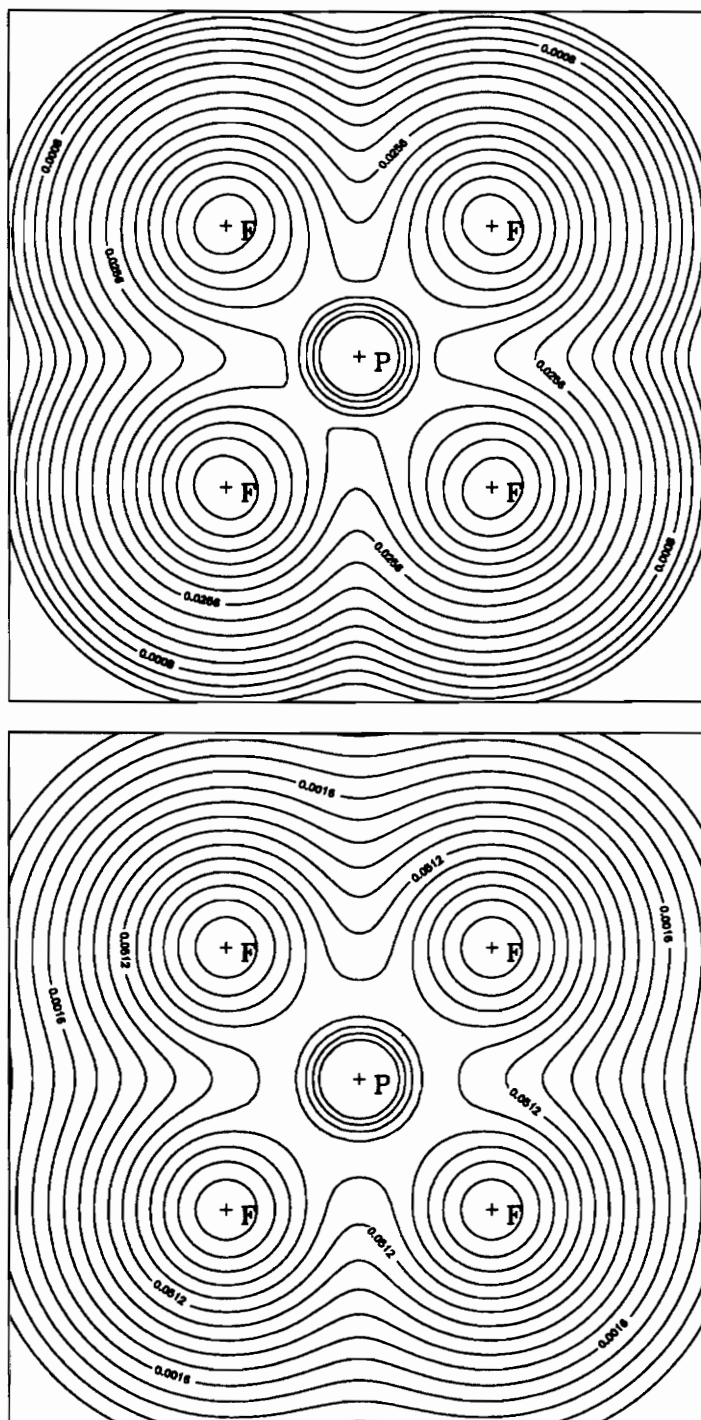
Figure B20. (a) Total electron density map for H_5NaF_6 and (b) promolecule electron density map for NaF_6. The contour interval is 0.0001, 0.0002, 0.0004, ...,e/b^3. The maps are 6.0 X 6.0Å.

Figure B21. (a) Total electron density map for H_4BeF_6 and (b) promolecule electron density map for BeF_6. The contour interval is 0.0001, 0.0002, 0.0004, ...,e/b^3. The maps are 6.0 X 6.0Å.

Figure B22. (a) Total electron density map for H_3AlF_6 and (b) promolecule electron density map for AlF_6. The contour interval is 0.0001, 0.0002, 0.0004, ...,e/b^3. The maps are 6.0 X 6.0Å.
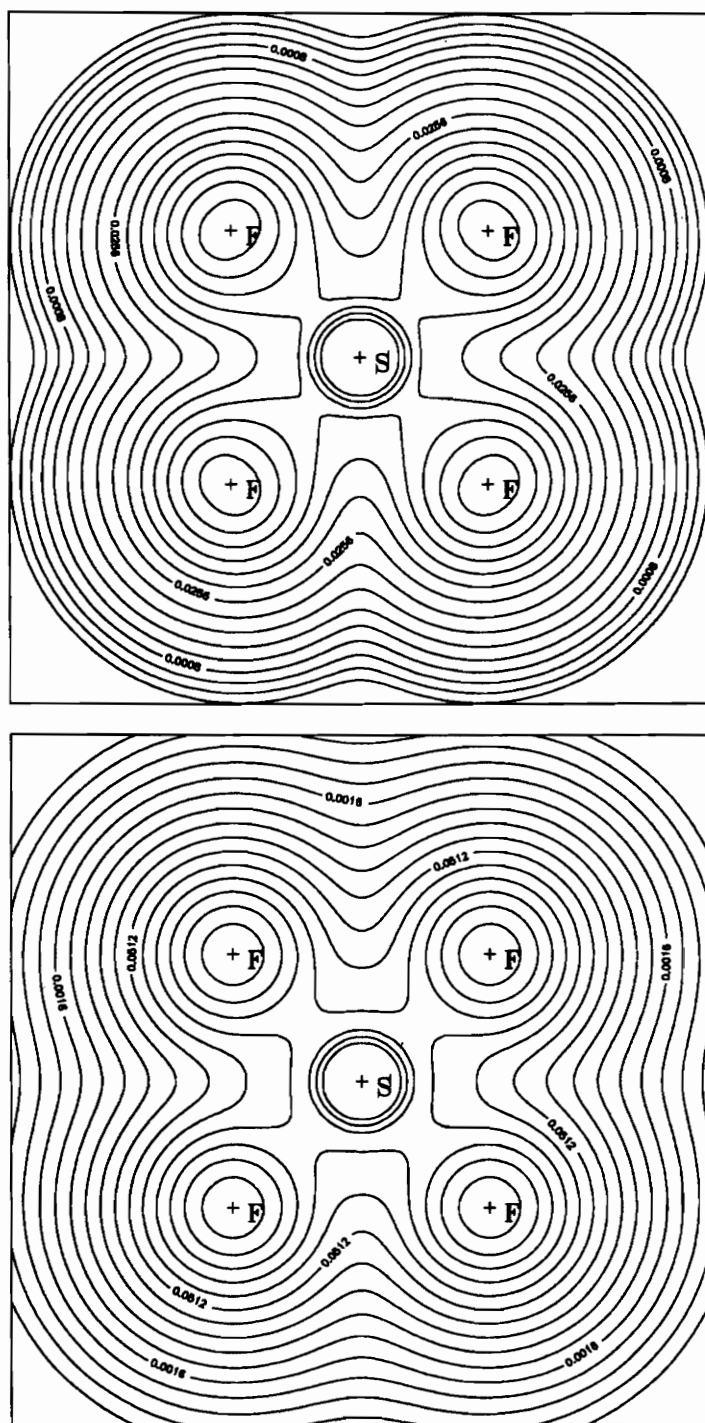
Figure B23. (a) Total electron density map for H_2SiF_6 and (b) promolecule electron density map for SiF_6. The contour interval is $0.0001, 0.0002, 0.0004, \ldots, e/b^3$. The maps are 6.0×6.0Å.

Figure B24. (a) Total electron density map for HPF_6 and (b) promolecule electron density map for PF_6. The contour interval is 0.0001, 0.0002, 0.0004, ...,e/b^3. The maps are 6.0 X 6.0Å.

Figure B25. (a) Total electron density map and (b) promolecule electron density map for SF_6. The contour interval is 0.0001, 0.0002, 0.0004, ...,e/b^3. The maps are 6.0 X 6.0Å.
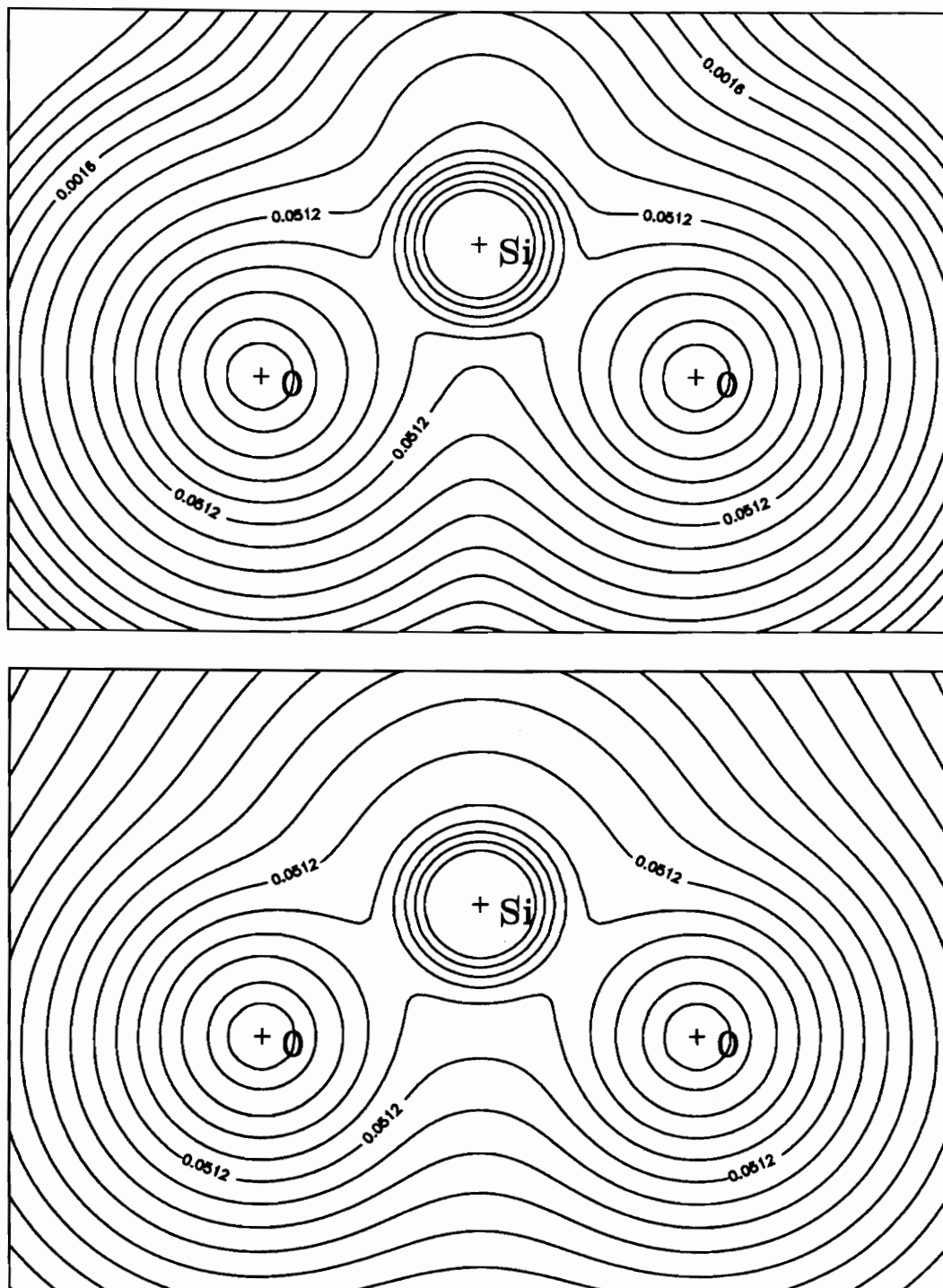
56

Figure B26. (a) Total electron density map and (b) promolecule electron density map for H_4SiO_4. The contour interval is 0.0001, 0.0002, 0.0004, ...,e/b^3. The maps are 6.0 X 4.0Å.

VITA

Jeffrey Scott Nicoll was born March 6, 1966, in Camden, New Jersey. A resident of South Jersey nearly all his life (except for 1969-71, during which he lived in South Korea), Jeff escaped and came to Blacksburg, Virginia, where he received a Bachelor of Science degree in geology from Virginia Polytechnic Institute and State University in 1989.